

OPEN ACCESS

EDITED BY
Daniel Menezes Blackburn,
Sultan Qaboos University, Oman

REVIEWED BY
Muhammad Adnan,
Chinese Academy of Sciences (CAS), China
Fayong Li,
Tarim University, China

*CORRESPONDENCE
Habib Ullah

☑ habib901@zju.edu.cn

RECEIVED 05 May 2025 ACCEPTED 03 June 2025 PUBLISHED 03 July 2025 CORRECTED 12 August 2025

CITATION

Ge Y, Ying K, Yu G, Ali MU, Idris AM, Shahab A and Ullah H (2025) A systematic review on machine learning-aided design of engineered biochar for soil and water contaminant removal.

Front. Soil Sci. 5:1623083. doi: 10.3389/fsoil.2025.1623083

COPYRIGHT

© 2025 Ge, Ying, Yu, Ali, Idris, Shahab and Ullah. This is an open-access article distributed under the terms of the Creative Commons Attribution License (CC BY). The use, distribution or reproduction in other forums is permitted, provided the original author(s) and the copyright owner(s) are credited and that the original publication in this journal is cited, in accordance with accepted academic practice. No use, distribution or reproduction is permitted which does not comply with these terms.

A systematic review on machine learning-aided design of engineered biochar for soil and water contaminant removal

Yunpeng Ge¹, Kaiyang Ying², Guo Yu², Muhammad Ubaid Ali³, Abubakr M. Idris^{4,5}, Asfandyar Shahab⁶ and Habib Ullah^{7,8*}

¹Guangxi Key Laboratory of Calcium Carbonate Resources Comprehensive Utilization, College of Materials and Chemical Engineering, Hezhou University, Hezhou, China, ²College of Environmental Science and Engineering, Guilin University of Technology, Guilin, China, ³College of Chemical Engineering, Huaqiao University, Xiamen, China, ⁴Department of Chemistry, College of Science, King Khalid University, Abha, Saudi Arabia, ⁵Research Center for Advanced Materials Science (RCAMS), King Khalid University, Abha, Saudi Arabia, ⁶School of Environmental Science and Engineering, Hainan University, Haikou, China, ⁷Department of Environmental Science, Zhejiang University, Hangzhou, Zhejiang, China, ⁸Innovation Center of Yangtze River Delta, Zhejiang University, Jiashan, China

The design and application of engineered biochar is crucial for removing contaminants from soil and water, yet its development and commercialization still depend on time- and labor-intensive experimental methods. Machine learning (ML) offers a faster alternative, but despite its growing use in biochar research, no review systematically covers ML-driven design of engineered biochar for large-scale contaminant removal. This work fills that gap by analyzing ML's role in optimizing biochar properties using pilot and industrialscale datal. We examine key biochar characteristics, including physical (e.g., surface area, pore volume), chemical (e.g., ultimate/proximate analysis, aromatization), electrochemical (e.g., cation exchange capacity, electrical conductivity), and functional group properties, and their optimization for various contaminants. With special attention on three mechanistic dimensions, this review offers the first thorough study of ML applications for designing biochars based on pilot and industrial-scale data: ML forecasts microporemesopore synergies controlling diffusion-limited adsorption of heavy metals (Pb²⁺, Cd²⁺); surface chemistry optimization - including oxygen functional group (-COOH, -OH); and electrochemical tuning - of redox-active sites for contaminant transformation. The paper emphasizes how ML models—such as Random Forest (RF) and Gradient Boosting Regression (GBR)-elucidate the nonlinear links between pyrolysis conditions (temperature, feedstock composition) and biochar performance. For adsorption, surface area and pore volume are distinctly important; in redox reactions for heavy metal removal, functional groups like C-O and C=O play vital roles. Unlike earlier studies mostly on the adsorption capacity of biochar, this work expands the scope to investigate how ML can customize biochar properties for optimal contaminant removal using interpretability tools like SHAP analysis. These instruments expose parameters including nitrogen-to-carbon (N/C) ratios and pyrolysis temperature in adsorption efficiency. The review also covers hybrid methods combining ML with molecular simulations (e.g., DFT) to link mechanistic knowledge with data-driven predictions. Emphasizing the need for

multidisciplinary collaboration, the review finally shows future directions for ML-driven biochar design, guiding fieldwork by pointing out shortcomings of present techniques and opportunities for ML.

KEYWORDS

machine learning (ML), engineered biochar, environmental remediation, adsorption, contaminants

Highlights

- ML forecasts the ideal characteristics of biochar for removing contaminants.
- Pyrolysis temperature dominates adsorption, according to SHAP analysis data.
- The redox reactions of heavy metals are controlled by oxygen functional groups.
- Pore structure-adsorption synergychars are controlled by feedstock chemistry.
- Mechanistic predictions are improved by hybrid ML-DFT models.

1 Introduction

Soil and water pollution, a critical global environmental issue intensified by rapid industrialization and population growth (1-3), poses significant threats to human health, disrupts ecosystems, and jeopardizes food safety (4, 5). Soil and water pollution remain pressing global concerns, with increasing evidence of their impact on ecosystems and human health. Nearly one-third of the world's soils are moderately to severely degraded as a result of erosion, nutrient depletion, acidification, and contamination, and more than 80% of wastewater is discharged into the environment untreated, according to the United Nations Environment Programme (6). The urgent need for efficient and sustainable remediation technologies like biochar-based systems—is highlighted by this concerning trend, especially when machine learning is added for targeted performance. Sustainable remediation techniques are needed to address these issues, and engineered carbonaceous materials like activated carbon and biochar are showing promise as remedies. Despite derived from the pyrolysis of biomass, they are different in significant regards: Biochar is a versatile adsorbent that can remove a variety of contaminants from soil and water. It is created by pyrolyzing organic feedstocks at temperatures between 300 and 700°C. Additionally, it improves soil quality and aids in carbon sequestration (7, 8). Because of its mineral concentration, heterogeneous pore structure, and abundance of surface functional groups (like -COOH, -OH), which boost microbial activity, water retention, and fertility, this is the best soil amendment (9). Because of its high adsorption capacity and porous structure, biochar can effectively remove both organic and inorganic contaminants from soil and water (8, 10–12). To create a more uniform, microporous structure with an exceptional surface area (500–3000 $\rm m^2/g)$, activated carbon is pyrolyzed at 600–900°C and then physically or chemically activated (e.g., steam, KOH). While this is ideal for the adsorption of contaminants in water treatment, it typically results in minimal benefits for the soil and increased production costs.

Recent studies have used several techniques including acid-base treatment, metal compound inclusion, steam activation, magnetization, heteroatom doping, and ball milling, which produce different adsorption results and mechanisms, so adjusting the properties of biochar to increase its efficacy as an adsorbent for particular contaminants or applications (13). However, the creation of synthetic biochar mostly depends on trial-and-error methods, sometimes laborious and useless (14, 15). Learning patterns from large datasets without the need of explicit programming or extensive experimentation helps machine learning (ML) especially to model and maximize the complex and nonlinear interactions between feedstock properties, pyrolyzed conditions, and the resulting biochar performance. This underlines the need of uniform evaluation criteria and the integration of artificial intelligence and machine learning to drive field developments.

The development of ML techniques has presented new opportunities for environmental use prediction and optimization of biochar performance. In view of their remarkable capacity to analyze intricate datasets, spot patterns, and predict outcomes, machine learning models are particularly well-suited to enhance biochar design (16, 17). Through machine learning, research has successfully predicted the properties and functionality of biochar, offering crucial insights into how changes in production conditions may affect the effectiveness of contaminant adsorption. Even though biochar and machine learning have been the subject of numerous recent studies, more research is still required. Most current research concentrate on specific, usually limited aspects of this relationship, so generating major knowledge gaps. Although Leng et al. (18) and Li et al. (19) carried out focused reviews focusing on specific biochar characteristics, such as pore volume, specific surface area, and nitrogen-containing functional groups, they do not address the general optimization of biochar for various types of pollutants or look into the broader implications of these characteristics in

environmental applications. For example, Wang et al. (20) carried out a mini-review on machine learning applications in biochar studies; however, it primarily offers a general overview without going into great detail about the design and optimization of engineered biochar for targeted contaminant removal. Although they provide useful analysis of particular biochar properties, they do not integrate the ways in which these attributes could be systematically targeted to improve biochar's effectiveness in various environmental contexts. The review by Zhang et al. (21) mostly concentrates on the use of biochar in anaerobic digestion rather than its application in soil and water contaminant removal, which is a crucial area for environmental remediation, similarly. This restriction emphasizes the need of a more thorough review covering the interaction between biochar characteristics and their performance in contaminant removal, which will finally guide future research and application strategies. Using these advanced computational tools allows researchers to rapidly produce more powerful biochar materials for environmental remediation.

In contrast to previous reviews that have mainly focused on the application of ML to engineer biochar properties for contaminant adsorption, this review broadens the scope to include a wider range of biochar characteristics and critically discusses how ML can be used not only to optimize biochar for specific contaminant removal but also to engineer biochar with tailored properties for diverse environmental and agricultural applications. This review thoroughly examines the application of ML in predicting and designing biochar properties, providing a detailed analysis of various biochar characteristics, including physical (specific surface area, total pore volume), chemical (ultimate/proximate analysis, aromatization degree), and electrochemical (cation exchange capacity, electrical conductivity, capacitance); and functional group properties.

This review is novel because it thoroughly examines how ML can be used to design biochar properties other than contaminant adsorption, providing insights into how ML could transform the biochar manufacturing process. By combining different machine learning algorithms and applying them to biochar research, the review demonstrates how ML can forecast and improve particular biochar characteristics, saving experimental time and expenses related to conventional trial-and-error methods. This more comprehensive viewpoint fills in important gaps in the body of literature, which makes it an essential addition to the field.

2 Review methodology

Multiple synonyms and Boolean operators were used in a methodical keyword search approach to guarantee thorough coverage of pertinent material. Expanded to include related terms such "artificial intelligence" OR "AI," "predictive modeling," "biochar modification," "biochar design," and "contaminant removal," the central search phrase was "machine learning" AND "engineered biochar." To maximize retrieval sensitivity, these terms were combined in several ways with Boolean operators (AND, OR). Among the example search strings were "machine learning" AND

"biochar"; "contaminant removal"; "artificial intelligence"; "Al"; "engineered biochar"; "predictive model"; AND "biochar adsorption". Limited to peer-reviewed journal publications released between 2009 and 2024, the searches were conducted in ScienceDirect, Web of Science, and Google Scholar. This strategy ensured the inclusion of studies addressing both the development of biochar materials and their optimization through machine learning tools.

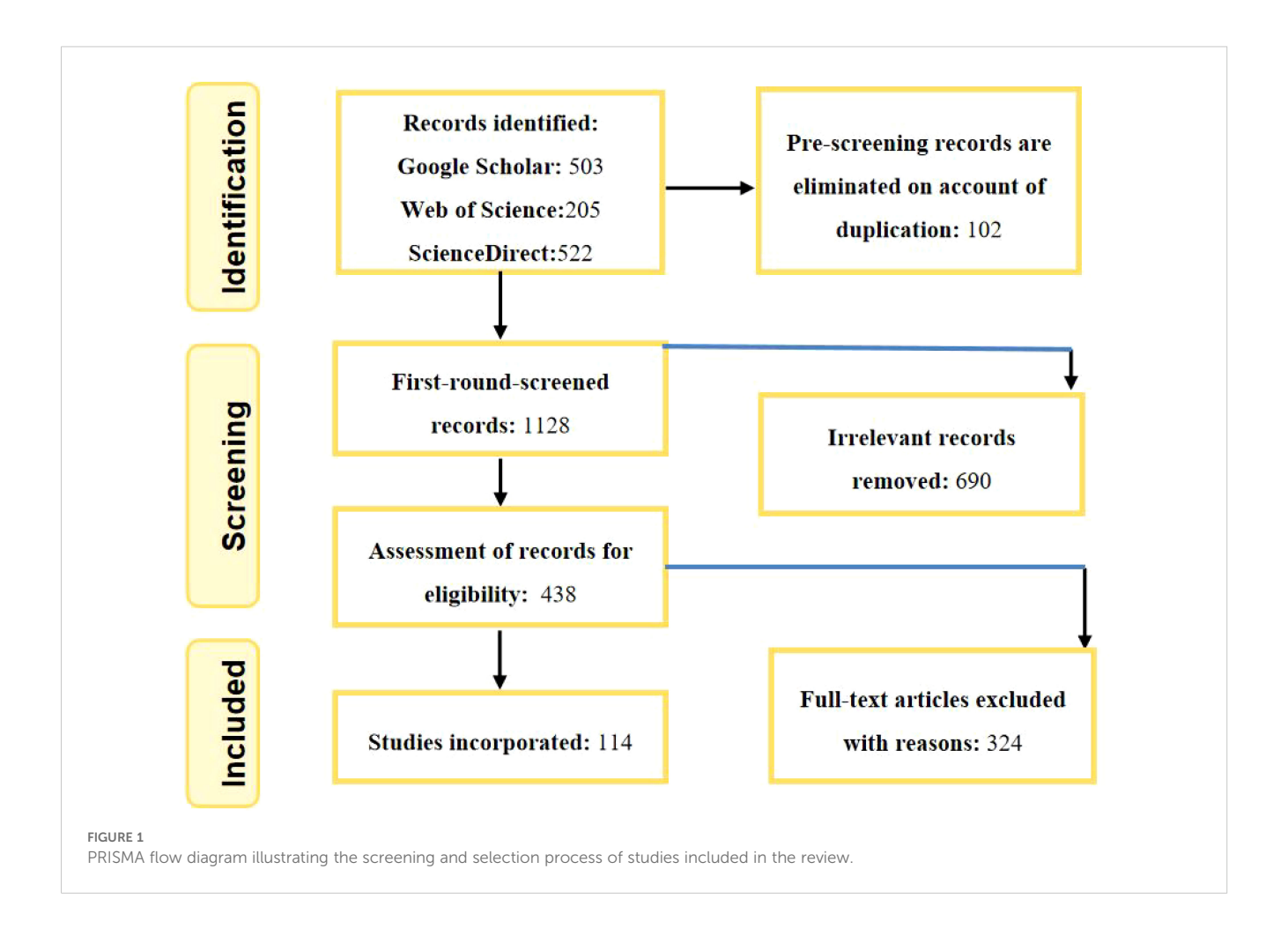
In total, 1,230 records were initially retrieved and exported to EndNote reference management software. After removing duplicates, 1,128 unique records remained. These were then screened based on titles and abstracts, resulting in the exclusion of irrelevant studies, including 324 review articles and conference proceedings. Finally, 1114 articles met the inclusion criteria and were analyzed in depth for this review. The full screening and selection process is summarized in Figure 1.

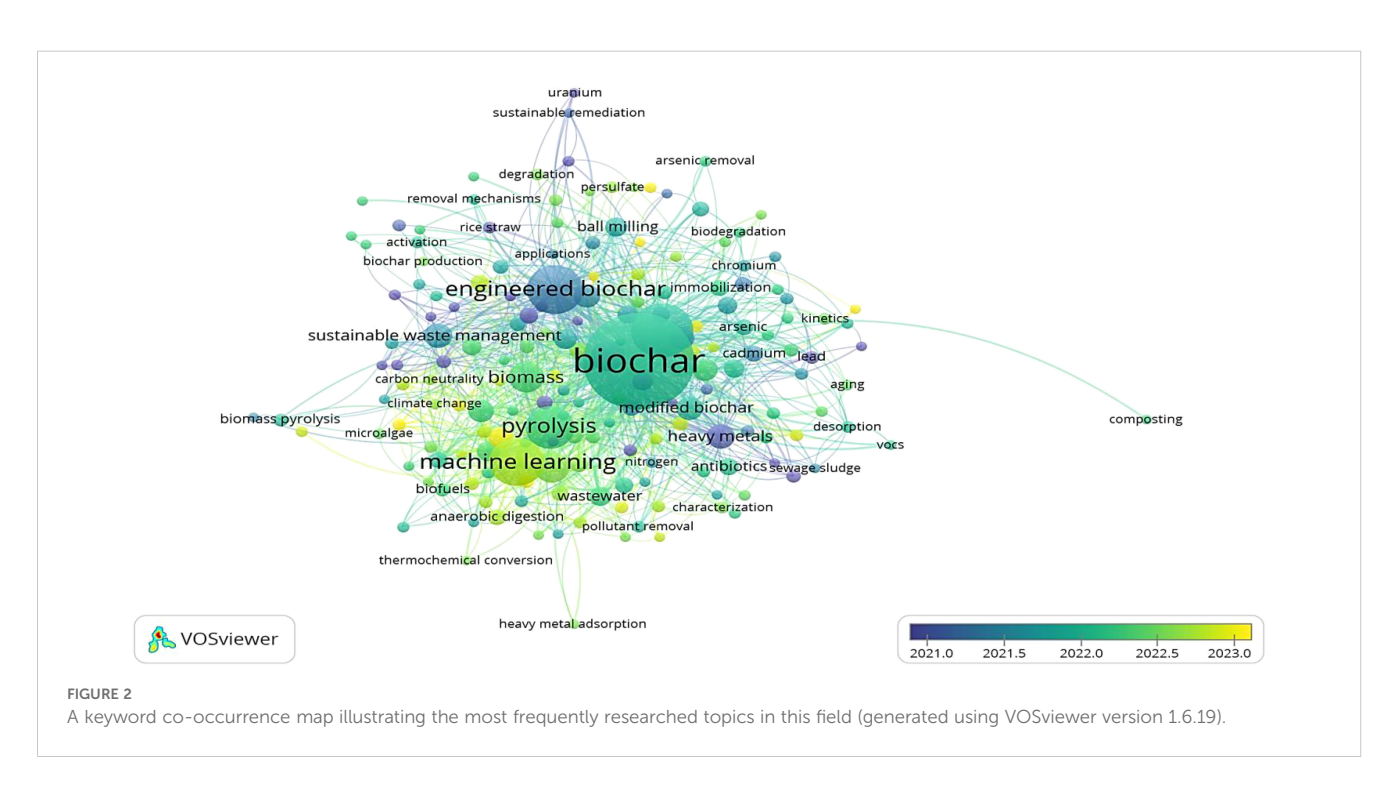
The significance of machine learning in biochar engineering is further supported by bibliometric mapping using VOSviewer software (version 1.6.19), as shown in Figure 2. This keyword cooccurrence map visually represents the most frequently researched terms related to machine learning and biochar. In the map, each node represents a keyword, with larger node sizes indicating higher frequency of occurrence in the literature. Different colors denote clusters of keywords that frequently appear together, revealing thematic groupings within the research domain. The proximity and thickness of the connecting lines between nodes reflect the strength of co-occurrence relationships, where closely connected nodes often appear in the same publications. This visualization highlights dominant topics such as "machine learning," "biochar properties," "adsorption," and "predictive modeling," underscoring the growing interdisciplinary convergence between data science and environmental material research.

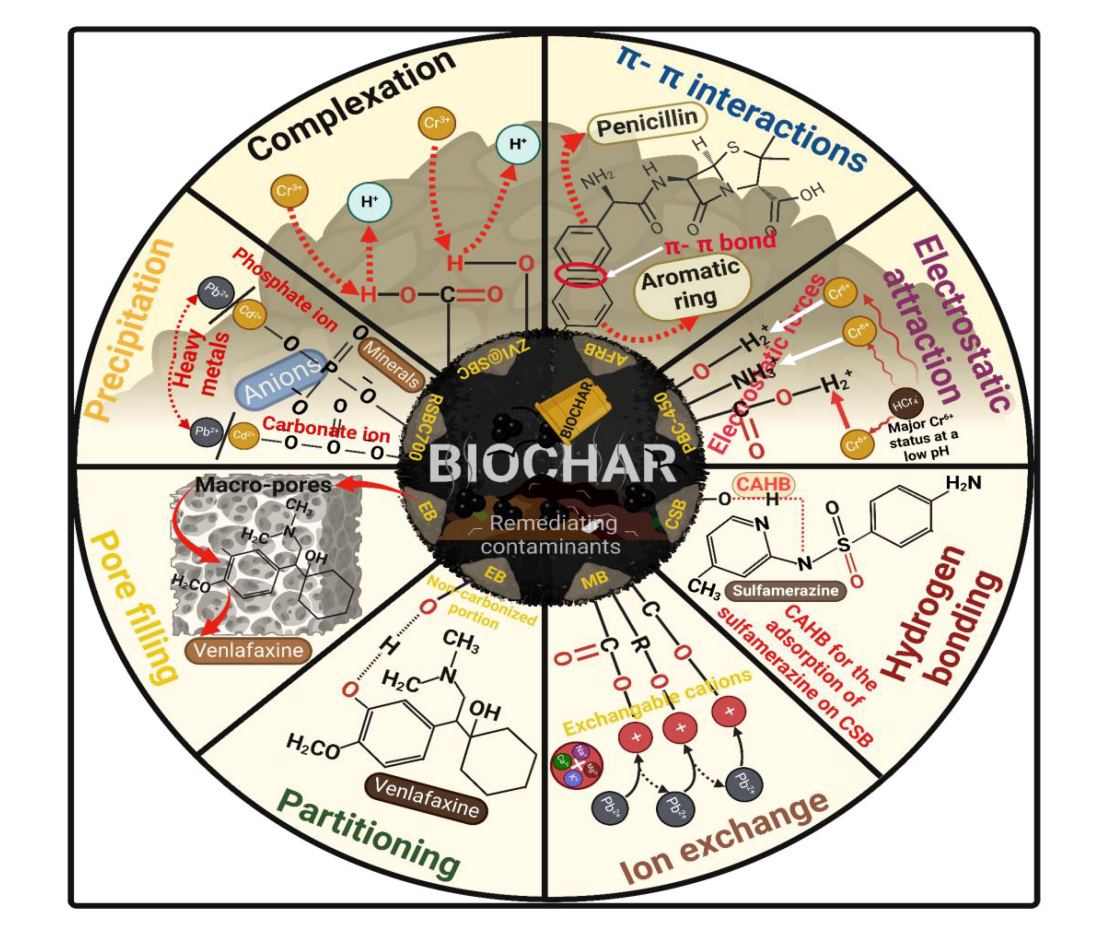
3 Biochar: a solution for remediating contaminants and its mechanism

Derived from carbon-rich materials by pyrolysis, biochar finds extensive use in environmental applications for the removal of pollutants from soil and water. Among these pollutants are organic compounds, heavy metals, pesticides, and dyes as well as drenches (22, 23). The type of feedstock, pyrolysis conditions, and the nature of the contaminants targeted affect its efficiency in eliminating these pollutants. Different mechanisms interacting with the pollutants—such as complexation, electrostatic attraction, hydrogen bonding, ion exchange, partitioning, pore filling, and precipitation—cause biochar to be versatile in remediation (Figure 3).

By means of particular ligand interactions, biochar binds metal ions in complexation (24). For wastewater, biochar made from municipal sludge, for example, efficiently removes hexavalent chromium (Cr(VI). The interaction of the metal and biochar surface changes the form of the metal, so reducing its toxicity (25). Likewise, in the adsorption of organic compounds, especially antibiotics and herbicides, π - π interactions are absolutely vital (26). These interactions made possible by biochar's aromatic structure







Various mechanism of contaminant's adsorption on biochar.

help to trap pollutants including penicillin and herbicides, so preventing their contamination of the environment (27).

Particularly in the removal of charged metal ions like chromate (28), electrostatic attraction is rather important. Depending on the pH of the solution and the pyrolyzed temperature of the biochar, the surface charge of biochar can draw in or repel some ions. For example, these electrostatic forces have made cauliflower stem biochar highly affine for chromate ions (29). The surface charge properties of biochar change with pH; this can either raise or lower its capacity to adsorb pollutants, particularly in acidic conditions. Hydrogen bonding is another mechanism in charge of biochar's ability to adsorb drugs and personal care products among other pollutants. Particularly the charge-assisted hydrogen bonds, these bonds aid highly soluble and mobile pollutants in their adsorption. A common PPCP, sulfamerazine, has shown notable efficiency in adsorbing biochar produced from corn straw, so stressing the part hydrogen bonds perform in environmental cleanup projects (30). Ion exchange is cation swapping from the biochar to the contaminant. This is particularly effective for heavy metals like lead (Pb), where the charged surface of biochar swaps ions with those in contaminated water (15). This process is made possible in part by the acidic oxygen-containing functional groups on the biochar surface—carboxyl, carbonyl, and hydroxyl groups—which ionize to swap with heavy metal ions or cationic organic pollutants. In biochar, partitioning is the dispersion of pollutants across its pores. The effectiveness of this process relies on the volatility of the biochar; pyrolyzed temperature affects this content. Usually, high concentration of volatile matter biochar performs better in adsorbing pollutants including pharmaceutical compounds (31). For instance, by means of partitioning, biochar generated from Eucalyptus pruning wastes has shown to effectively adsorb pharmaceutical contaminant venlafaxine (32). Another method whereby pollutants occupy the micropores and mesopores of biochar is pore filling. Higher pyrolyzed temperatures—which produce more micropores—cause the specific surface area of the biochar to rise, so increasing the adsorption capacity. Research on biochar generated from Eucalyptus for the adsorption of venlafaxine has exposed this mechanism is essential for the elimination of organic pollutants (31, 32).

Lastly, the developed solid precipitates on biochar surface offer the means of removing heavy metals from aqueous solutions. For metals including cadmium (Cd) and lead (Pb) this approach has shown good success (Figure 3). Large concentrations of Cd and Pb discovered deposited on the biochar following treatment have made biochar produced from rice straw highly successful in precipitating and removing these metals from water (33).

When all factors are considered, a combination of treatment techniques interacting with a wide spectrum of pollutants determines whether biochar can remove contaminants in soil and water. Its adaptability and efficiency make it a great tool for addressing environmental damage. Its uses can be changed to fit a range of pyrolyzed conditions and feedstocks for best effects.

4 Machine learning

4.1 Overview of ML

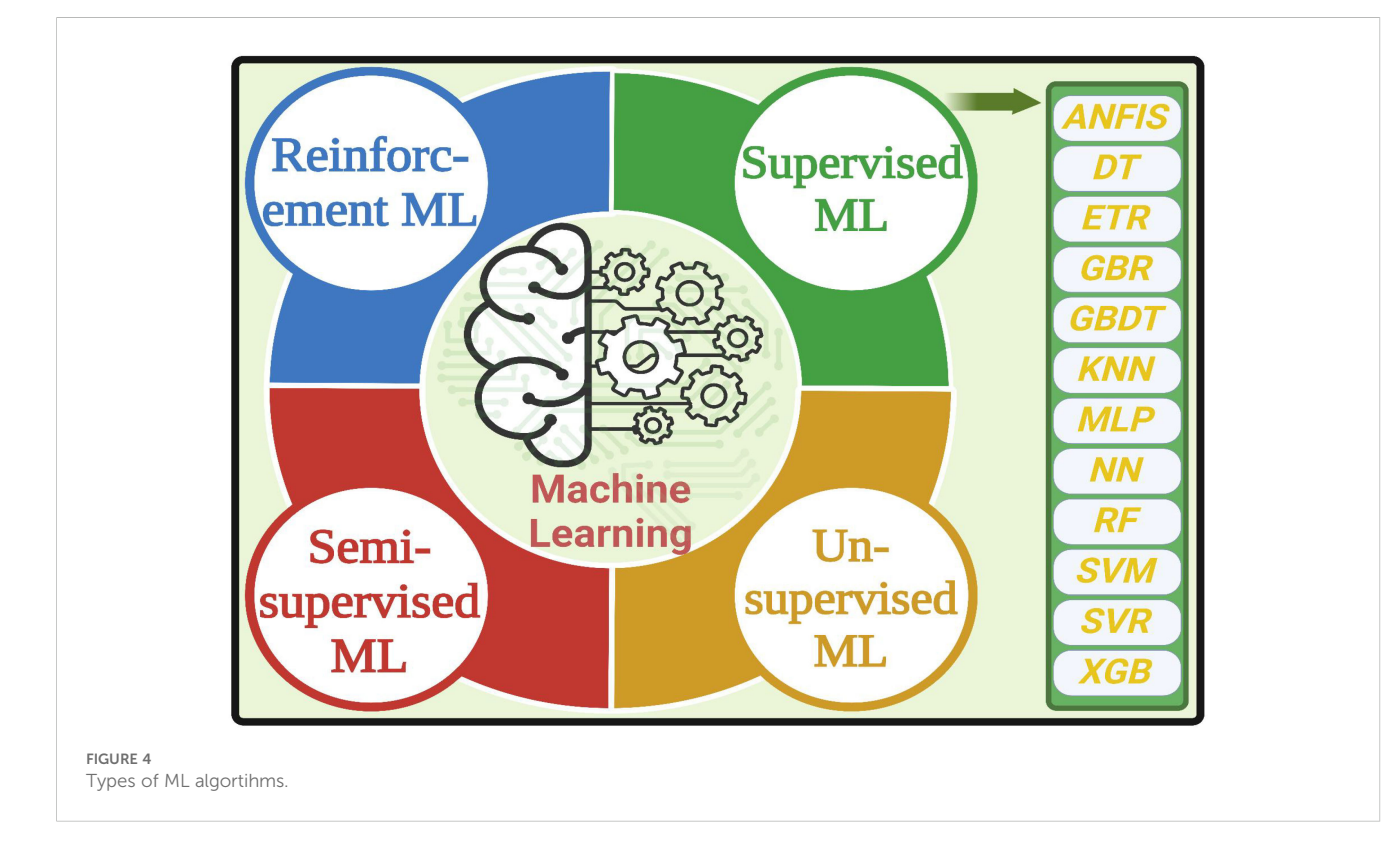
Within artificial intelligence (AI), ML is a subset aimed at creating models allowing computers to learn from data to generate predictions or decisions (34). ML is a great tool for simulating challenging processes by means of accurate predictions free from major testing (35, 36) by modeling mathematical relationships between inputs and outputs. This capacity significantly reduces the load of experimental studies and the time costs (16). While offering more scalability and flexibility, ML gives great accuracy in creating predictions top priority over traditional statistical methods that focus on deriving relationships between variables. (37).

As shown in Figure 4, ML techniques applied in this field include supervised, unsupervised, semi-supervised, and reinforcement learning methods (38, 39). For example, following training models with labelled data, supervised learning separates further into classification and regression tasks (40). Unsupervised learning stresses on clustering and analysis of unlabeled datasets while semi-supervised learning combines both approaches. In biochar research,

for example, supervised learning can be used with known experimental data to classify feedstock types depending on their physicochemical properties or predictability of adsorption capacity for specific heavy metals. Here we often apply models such as Random Forest or Support Vector Machines. Conversely, unsupervised learning deals with unlabeled data such that the model finds hidden patterns or groupings free from predefined categories. Cluster adsorption efficiencies across many biochar samples can be utilized for natural groupings based on performance or to find relationships between feedstock properties and adsorption behavior for biochar using unsupervised learning. Many times used in such research are k-means or hierarchical clustering techniques. Reinforcement learning guides models to maximize results by means of interaction with their surroundings (41).

Although recent developments show that deep learning (DL) models and hybrid systems offer significant advantages in capturing complex feature interactions and uncovering hidden patterns, they often function as "black boxes (42)," so providing limited insight on how particular predictions are made despite their promise in analyzing huge datasets. GBR and RF still rule the literature due to their great performance in handling non-linear, high-dimensional datasets. Moreover, applying features learnt in one environment to several problem domains helps to increase model adaptation (43). Particularly in domains like image processing and speech recognition, DL technology is developing rapidly.

A class of feedforward artificial neural networks, Multilayer Perceptrons (MLPs) have shown great predictive accuracy for modeling adsorption capacity and biochar surface properties. In the 2022 Da et al. study, a two-layer MLP outperformed SVR, RF, and linear models in estimating uranium adsorption, so obtaining



 $R^2 \approx 0.99$ and RMSE = 3.75. When the relationship between input features (e.g., feedstock composition, pyrolysis conditions) and output targets (e.g., surface area, O/C ratio) is highly non-linear and not easily captured by conventional tree-based methods, MLPs are especially useful.

Furthermore under increasing investigation in materials science for microstructural pattern analysis or spectroscopic data related to biochar surfaces are convolutional neural networks (CNNs), widely used in image analysis. Although they are not yet widely used in biochar research, CNNs have potential in analyzing graphical input data such as SEM images or adsorption isotherms, which are typically underused in conventional machine learning pipelines.

Moreover shown to be better than both ANN and standalone ML models in some predictive tasks are hybrid models including Adaptive Neuro-Fuzzy Inference Systems (ANFIS). For example, Abdi et al. (44) estimated the electrical conductivity of compost improved by biochar-enhanced $R^2=0.999$, RMSE = 0.002) with better accuracy of ANFIS over ANN. Particularly useful when both high accuracy and rule-based insight are sought for is ANFIS, which blends the learning capacity of neural networks with the interpretability of fuzzy logic.

Future research should also consider ensemble learning frameworks such stacking (meta-modeling) and bagging into account to aggregate predictions from several base learners to improve robustness and generalization especially when dealing with heterogeneous datasets derived from different feedstocks and experimental settings. This review of ML ideas and advancements emphasizes its applicability in domains including environmental science and biochar research, where it helps to forecast results and maximize procedures, so promoting more sustainable practices.

4.2 Evaluation metrics for ML models

The accuracy and effectiveness of the regression models can be evaluated by using the coefficient of determination (R²), the mean squared error (MSE), and the root mean squared error (RMSE) (45) variables. The coefficient of determination, also known as R², is a statistical measure that can range from 0 to 1 and is used to determine the percentage of variation that can be attributed to the model. R² values that are higher and closer to 1 point indicate that the model is a better fit to the data. According to Henseler et al. (46), values that fall between 0.25 and 0.75 are categorized as moderate, values that fall below 0.25 are regarded as weak, and regression models that obtain an R2 value of 0.75 are regarded as being rather predictive. Other than R2, MSE is a measurement of the average squared difference between the values that were actually observed and those that were projected; RMSE is the square root of MSE. The root mean square error (RMSE) is useful because it highlights the impact of significant data errors.

Due to the fact that they provide an insightful analysis of the predictive capacity of the model as well as the degree of prediction errors, R^2 and RMSE were utilized the majority of the time when evaluating the models (45).

5 ML for predicting and designing biochar properties

With desired properties, ML is progressively a useful tool in biochar research (19, 47). By differentiating the complex interactions among biochar properties, manufacturing techniques, and performance (48), machine learning models significantly help in this field. When predictive ML models including biochar material design incorporate optimization techniques instead of the traditional trial-and-error method, ML drastically lowers laboratory effort, cost, and time (19). Simulating biochar features (49) has effectively predicted performance depending on many factors by means of regression and other supervised learning techniques. Ultimately, including machine learning (ML) into biochar research is inspiring innovation, enabling more environmentally friendly and efficient biochar production, and so extending its applications in agricultural and environmental spheres. Its capacity to maximize biochar production methods by means of particularly bibliometric approaches highlights even more its potential (50).

Furthermore, ML is revolutionary for predicting the properties of biochar by screening biomass and creating pyrolyzing conditions (35). Yargicoglu et al. (51) state that the feedstock and production method affect the physical, chemical, and electrochemical characteristics of biochar. Consequently, whereas input parameters could include biomass characteristics such as proximal composition and elemental composition of feedstock, volatile matter, ash, fixed carbon, and moisture content, pyrolyzed conditions include pyrolytic temperature, retention time, and heating rate; hence, in our review article, various physical, chemical, and electrochemical properties are taken as output or predicted parameters. Table 1 summarizes the uses of several supervised learning systems for the prediction of physical, chemical, and electrochemical characteristics of biochar.

5.1 Physical properties

5.1.1 Specific surface area

The main factor influencing biochar's effectiveness as a carbon material in a variety of applications, such as energy storage, CO2 and H₂ adsorption, catalysis, and contaminant removal, is its specific surface area (58, 59). Liang et al. (60) declared biochar to be an effective material for the adsorption of contaminants due to its high specific surface area. Although, Leng et al. (52) consider the production of biochar with a preferred specific surface area to be a difficult endeavor. Thus, the authors develop a ML model to predict and optimize the specific surface area of biochar made from maize, rice, and sawdust, using pyrolysis condition (temperature), biomass composition (Ash, fixed carbon, moisture, volatiles), biomass elemental composition (C content, H content, O content, N content), biomass biochemical composition (cellulose, hemicellulose and lignin content), and activation conditions (activation temperature, heating rate and residence time as input variables. It's important to note that both the diversity of biomass

TABLE 1 Various supervised ML models for predicting biochar physical, chemical and electrochemical features.

Feedstocks	Input parameters	Target	ML	Data	Predictive performance		Findings	Reference
		(output)	algorithms	size	R ² (Train/Test)	RMSE (Train/Test)		
Corn husk, rice husk, sawdust	Pyrolysis condition (temperature), Biomass composition (Ash, fixed carbon, moisture, volatiles), Biomass elemental composition (C content, H content, O content, N content), Biomass biochemical composition (cellulose content, hemicellulose content and lignin content), Activation conditions (activation temperature, heating rate and residence time)	Specific surface area	GBR RF	68 68	1.00/1.69 0.99/0.85	0.91/39.65 14.90/51.85	ML successfully predicted and optimized the biochar specific surface area	Leng et al. (52)
Agro, softwood and hardwood, marine waste, macroalgae	Pyrolysis condition (temperature), biomass composition (ash, fixed carbon, moisture, volatiles), biomass elemental composition (C content, H content, O content, S content, N content), biomass biochemical composition (cellulose content, hemicellulose content and lignin content), activation conditions (activation temperature, heating rate and residence time)	Specific surface area	DT KNN RF	292 292 292	0.61/NI* 0.55/NI* 0.80/NI*	7.01/NI* 9.15/NI* 4.32/NI*	RF performed better than DT and KNN	Hai et al. (45)
Bran, corn stalk, husk, peanut shell, rice sawdust, and straw stalk	Pyrolysis condition (temperature), Biomass composition (Ash, volatiles), Activation conditions (activation temperature, heating rate and residence time)	Specific surface area	GBR RF	169 169	0.99/0.92 0.94/0.91	0.02/46.53 31.48/48.78	GBR model generated more accurate predictions compared to the RF model	Li et al. (19)
Corn husks, corn cobs, rice straw, sugarcane bagasse, wheat straw, and wood waste	Biomass composition (Ash, fixed carbon, moisture, volatiles), Biomass elemental composition (C content, H content, O content, N content), Biomass biochemical composition (cellulose content, hemicellulose content and lignin content), Activation conditions (activation temperature, heating rate and residence time)	Specific surface area	GBDT RF XGB	258 258 258	0.95/0.93 0.93/0.77 0.95/0.92	0.70/216.9 0.89/413.2 0.84/239.3	GBDT presented the better prediction accuracy and generalization ability than the RF and XGB.	Li et al. (53)
Bamboo chips, bagasse, corn stover bark, coconut shells, corn stover, digestate, food waste digestate, municipal biosolid waste, pine chips, palm kernel shells, rice husk rice straw, swine manure, soybean oil cake, walnut shells, yak manure	Biomass type, pyrolysis condition (temperature), Biomass composition (ash, fixed carbon, volatiles), Biomass elemental composition (C content, H content, O content, N content), Activation conditions (activation temperature, heating rate and residence time)	Specific surface area	GBDT RF XGB	258 258 258	0.98/0.87 0.97/0.81 0.96/0.92	32.31/57.32 31.90/52.14 32.11/45.21	XGB performed significantly for predicting specific surface area for the biochar	Zhou et al. (54)
Bran, corn stalk, husk, peanut shell, rice sawdust, and straw stalk	Pyrolysis condition (temperature), Biomass composition (Ash, fixed carbon, moisture, volatiles), Biomass elemental composition (C content, H content, N content, O content, S content)	Total pore volume	GBR RF	152 152	0.99/0.91 0.96/0.90	0.01/0.06 0.04/0.06	GBR models trained in this work have better performance compared with RF models	Li et al. (19)

TABLE 1 Continued

Feedstocks	Input parameters	Target	ML	Data	Predictive performance		Findings	Reference
		(output)	algorithms	size	R ² (Train/Test)	RMSE (Train/Test)		
Corn husks, corn cobs, rice straw, sugarcane bagasse, wheat straw, and wood waste	Biomass composition (Ash, fixed carbon, moisture, volatiles), Biomass elemental composition (C content, H content, N content, O content), Biomass biochemical composition (cellulose content, hemicellulose content and lignin content), Activation conditions (activation temperature, heating rate and residence time)	Total pore volume	GBDT RF XGB	258 258 258 258	0.91/0.83 0.90/0.77 0.90/0.86	0.22/216.9 0.26/413.2 0.20/239.3	GBDT presented the better prediction accuracy and generalization ability than the RF and XGB.	Li et al. (53)
Agricultural and forestry wastes, sewage sludge and algae	Biomass composition (Ash, fixed carbon), Biomass elemental composition (molar concentrations of C, H, O, N as well as wt % of C, H, O, N). Biochar physical characteristics (particle size, surface area, ash yield, atomic ratio), Biochar chemical feature (pH)	Cation exchange capacity	GBR	353	0.94/0.74	2.14/3.44	GBR outperformed RF	Shen et al. (17)
Cooked rice, coco peat, vegetable residues (cabbage, squash, lettuce)	Biomass elemental composition (Wt % (C/N)), composting time, fresh inlet air rate	Electrical conductivity	RF ANN ANFIS	353 198 198	0.80/0.82 NI*/0.925 NI*/0.999	4.27/2.39 NI*/0.073 NI*/0.002	ANFIS provided a more accurate prediction in comparison with ANN	Abdi et al. (44)
Mango seed husk	Activation conditions (activation time, activation temperature), Biochar physical condition (specific surface area, pore volume, average pore diameter and current density)	Capacitance	DT MLP SVR	NI* NI* NI*	0.94/NI* 0.99/NI* 0.98/NI*	18.08/NI* 4.1/NI* 4.5/NI*	MLP provided insight on designing carbon materials for developing carbon-based electrodes for energy storage	Wickramaarachchi et al. (55)
Aloe vera, banana peel wastes, bean dergs, cotton, corncob, corn husk, Chinese oil palm kernel shell, cauliflower, Camellia oliefera shell, fermented rice, garlic skin, human hair lotus leaf, lotus seedpods, parasol fluff, pine tree powder, pine cone, Perilla frutescens, potato waste, rice straw, spruce, sakura petals, tobacco rods, waste coffee grounds, and willow catkins	Activation conditions (activator type, activation time, activation temperature), Biochar physical condition (specific surface area), Biomass elemental composition (Wt % of C/O, C/N).	Capacitance	ANN DT RF XGB	9 9 9 9	0.31/0.20 0.98/0.97 0.89/0.56 0.99/0.98	78.96/102.40 13.42/15.00 32.71/67.95 6.32/12.37	Extreme gradient boosting had best prediction effect on the electrical capacity of biochar	Yang et al. (56)
Corn straw	Biomass composition (Ash, fixed carbon, mass ratio of urea-to-biochar, mass ratio of potassium-to-biochar in the potassium activator), Biomass elemental composition (C content, H content, O content, N content),	Capacitance	ETR GBR RF	157 157 157	0.99/0.92 0.93/0.90 0.99/0.93	NI* NI* NI*	GBR performed better than ETR and RF.	Sun et al. (57)

Feedstocks	Input parameters	Target	ML	Data	Predictive performance	vrmance	Findings	Reference
		(output)	algorithms size	size	R ² (Train/Test)	R ² (Train/Test) RMSE (Train/Test)		
	Activation conditions (activation temperature, activation time, and heating rate)							
Com husk, rice husk, sawdust	Pyrolysis condition (temperature), Biomass composition (Ash, fixed carbon, moisture, volatiles), Biomass elemental composition (C content, H content, O content, N content), Biomass biochemical composition (cellulose content, hemicellulose content and lignin content), Activation conditions (activation temperature, heating rate and residence time)	Functional	GBR RF	67	0.90/0.65	0.38/0.79	GBR outperformed RF for N-char prediction.	Leng et al. (52)
Coffee grounds, Chipboard, sewage sludge	Biomass elemental composition (Wt % of C content, H content, S content, N content), pyrolysis conditions (temperature, heating rate and residence time)	Functional	GBR	150	0.99/0.90	2.25/8.25	Both ML models significantly optimized pyrolysis temperature for predicting and engineering biochar N-functional groups.	Leng et al. (18)
*= Not informed.								

species and the complex biochemical composition within the same type lead to distinct pyrolysis product properties when processing wood, bark, or leaves individually or together (61). The prediction of specific surface area was evaluated using RF and GBR models on 68 data sets, with 20% testing and 80% training for avoiding the overfitting of the trained model. The GBR and RF models predicted biochar's specific surface area with R² (1.00, 0.99, respectively) and RMSE (0.91, 14.90, respectively) (Table 2). When R² and RMSE values are considered, the RMSE of the GBR model is noticeably smaller than that of the RF model. Therefore, the GBR model's predictions are more accurate in relation to the actual values, thus indicating its superior performance in comparison to the RF model. Furthermore, ash and temperature are the two most important factors in predicting the specific surface area of biochar because ash has a significantly negative effect on the surface area of biochar, especially when the ash content is less than 2%; this negative impact is primarily due to pore formation during pyrolysis, which is closely related to the release of volatile matter. Higher ash concentration usually clogs many pores, so reducing the total specific surface area (72). Apart from the ash content, the pyrolysis temperature is quite crucial for the prediction of specific surface area of biochar in such a way that increasing temperature facilitates the conversion of amorphous carbon to crystalline carbons, so removing more volatiles and producing cracks in biochar. These cracks create sparse regions, fostering the development of more pores and resulting in a significant increase in specific surface area.

Using ML algorithms—including linear regression (LR), support vector machines (SVM), random forests (RF), and multilayer perceptron neural networks (MLP-NN)—Da et al. (73) predicted uranium adsorption behavior on biochar. According to their findings, not the chemical composition but rather the specific surface area (SA) of biochar determines uranium adsorption (73). Though several factors affect uranium adsorption on biochar, their respective effects differ rather significantly. Da et al. found, using permutation feature importance with the two-layer MLP model, specific surface area as the most important physical characteristic, in line with conventional adsorption theories. Their work evaluated important biochar properties including specific surface area (SA), total pore volume (V_{Tot}), average pore diameter (Dav), oxygen-to- carbon ratio (O/C), and carbon content (C). Adsorption capacity is much raised by increasing the specific surface area beyond 300 m²/g; increases beyond 800 m²/g have less effect on uranium adsorption.

Jiang et al. (74) used a whole approach combining K-fold crossvaluation, Optuna, machine learning, and SHAP analysis to investigate elements impacting ciprofloxin (CIP) adsorption by biochar. The CIP adsorption capacity of biochar and its specific surface area were found to have a positive correlation in the study. A specific surface area of approximately 915.6 m²/g marked a threshold above which adsorption capacity increased significantly. This finding aligns with the understanding that a larger surface area provides more adsorption sites, enhancing the biochar's ability to retain pollutants. It is important to note that the surface area contributed a mere 2% to the adsorption efficiency of six heavy metals when analyzed comprehensively across the 353 datasets from the adsorption processes (75), as depicted in Figure 5.

Materials	Feedstock	Pyrolysis temperature (°C)	Contaminants	Application dose (g/L or Kg)	Medium	Removal capacity (g/Kg or L)	Adsorption efficiency (%)	Mechanism involved	References
AFRB	Penicillin fermentation residue	800	Penicillin	80	Water	44.05	93.32	π- $π$ interactions	Wang et al. (27)
MB	Microalgae reside (Spirulina sp.)	600	Pb	150	Water	154.5	74.40	Ion exchange	Yang et al. (62)
EB	Eucalyptus	500	Venlafaxine	2.8	Wastewater	2.65	>99	Partitioning, pore filling	Puga et al. (32)
M-BC	Maize straw	900	Perfluorobutyric acid	50	Wastewater	2.54	>91	Partitioning	Liu et al. (63)
CSB	Corn straw	300	Sulfamerazine	0.05	Water	NI*	>99	Hydrogen bonding	Li et al. (19)
ZVI@SBC	Municipal sludge	450	Cr	1.5	Wastewater	150.83	NI*	Complexation	Yang (25)
PBC-450	Cauliflower stem	450	Cr	5	Wastewater	64.10	NI*	Complexation, Electrostatic attraction	Chanda et al. (29)
SCB	Sugarcane bagasse	500	Fluoride	0.183	Water	NI*	86.20	Electrostatic attraction, ion exchange	Girkar et al. (11)
SBEB	Stem bark of Eucalyptus	650	Cr, Pb	0.12	Water	238.12 for Cr and 175.02 for Pb	NI*	Electrostatic attraction	Mustapha et al. (64)
EWB	Eucalyptus wood waste	450	Anthracene	0.4	Water	NI*	98.41	Hydrogen bonding	Ilyas et al. (65)
В7	Corn cob	700	Acetaminophen, amoxicillin	1	Wastewater	64.99 for acetaminophen, 26.62 for amoxicillin	NI*	Pore filling	Varela et al. (66)
VI-BC	Vateria indica fruits	200	2,4- Dichlorophenoxyacetic acid	0.3	Waterbodies	NI*	91.67	π- π interactions	Vinayagam et al. (67)
FS-PNBC	Fish scale and pine needle	600	Ciprofloxacin	60	Water	27.97	NI*	Electrostatic attractions, π - π interactions, Hydrogen bonding	Lu and Zhao (68)
RSBC700	Rice straw	700	Cd, Pb	1	Wastewater	62.45 for Cd, 167.49 for Pb	NI*	Precipitation	Liu et al. (33)
To-B, Ri-B, Ru-B	Tobacco stem, Rice husk, Rubber wood	750	Cd	20	Soil	3.07 (To-B), 2.42 (Ri-B), 3.22 (Ru-B)	NI*	Electrostatic attractions, precipitation	Wang et al. (69)
RSS	Reed straw	800	Methylene violet dye	1	Water	92.6	NI*	Hydrogen bonding, Pore filling	Tomin et al. (70)
HTBC	Egyptian doum palm fruit shells	500	Methyl orange dye	0.01-0.07	Water	264.922	NI*	Electrostatic attractions, π - π interactions, Hydrogen bonding, Pore filling	Tcheka et al. (71)

^{*=} Not informed.

More studies regarding ML algorithms for predicting biochar's specific surface area are summarized in Table 2.

5.1.2 Total pore volume

ML offers enormous potential for engineering biochar materials with large pore volumes. In this regard, Li et al. (19) used GBR and RF to improve pyrolysis conditions and biomass mixing ratios for designer biochar. In that scenario, six kinds of biomass (bran, maize stalk, husk, peanut shell, rice sawdust, and straw stalk) were used to predict the total pore volume of biochar using the best ML models. As a result, in this study, 80% of the dataset was selected at random to train GBR and RF models, with the remaining 20% used for testing. The higher the R² and the lower the RMSE, the more accurate the prediction and performance of the trained model. In this sense, GBR predicted biochar total pore volume more accurately without overfitting ($R^2 = 0.99$ and RMSE = 0.01) than RF ($R^2 = 0.96$ and RMSE = 0.04). Among various input parameters (pyrolysis condition (temperature), biomass composition (ash, fixed carbon, moisture, and volatiles), and biomass elemental composition (C content, H content, N content, O content, and S content), temperature is almost linearly and positively related to total pore volume in the temperature range of 350-800°C; however, temperatures less than 350°C have little effect on pore volume, and temperatures greater than 800°C may lead to no increase in pore volume. The release of volatile compounds from the surface of biomass particles causes the creation of pores. Higher temperatures improve volatilization and may lead to the creation of additional pores on biochar (19).

Jiang et al. (74) revealed a strong positive correlation between pore volume and adsorption capacity of ciprofloxacin (CIP). When pore volume surpasses 0.1 cm³/g, a significant majority of SHAP values become positive, indicating a substantial contribution of pore volume to the adsorption process. This aligns with the established understanding that increased pore volume equates to a greater

number of accessible adsorption sites (76), thereby enhancing the overall adsorption capacity of the biochar for contaminants.

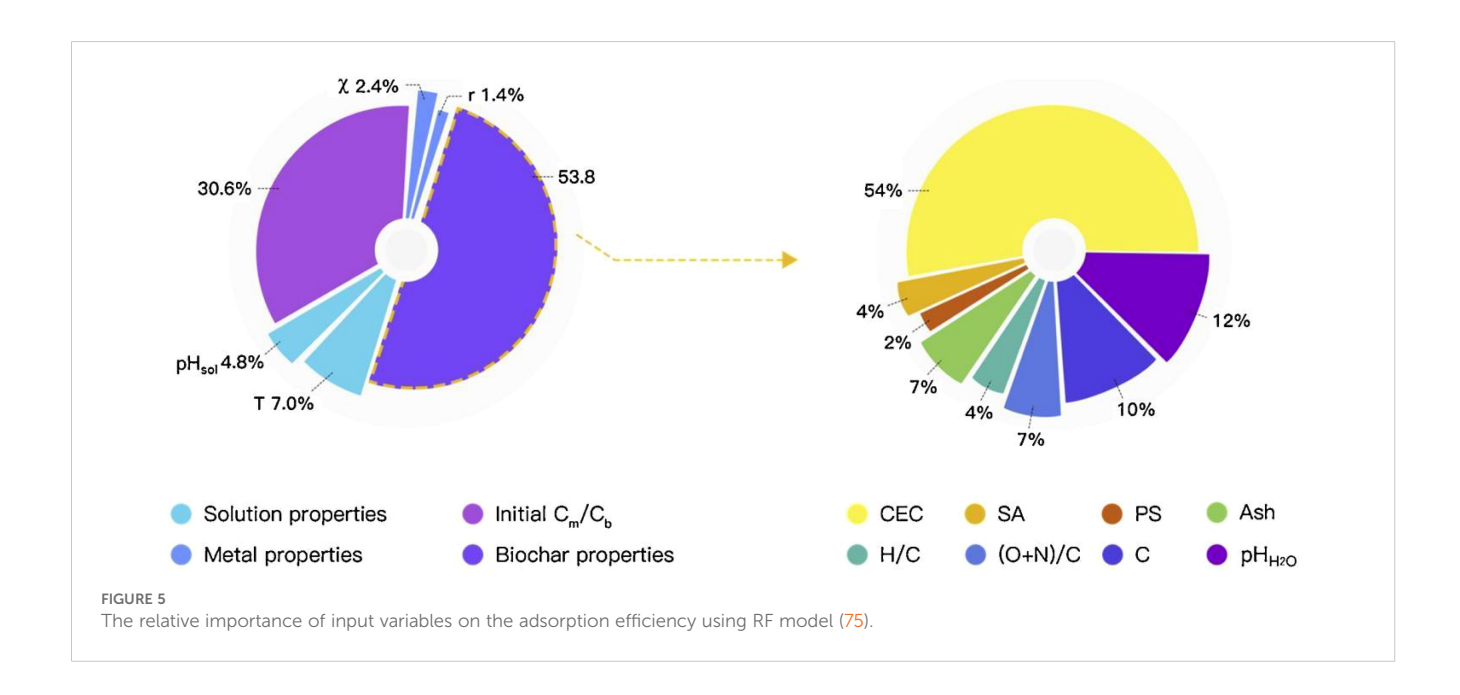
6 Chemical and electrochemical properties

6.1 Ultimate/proximate analysis

Various ML techniques have been successfully employed to predict the properties of biochar, including its C, H, N, O, fixed carbon (FC), volatile matter (VM), and ash content (77). Typically, biochar is composed primarily of carbon, which constitutes 65 to 90 wt%, along with smaller amounts of hydrogen, oxygen, ash, and trace elements of nitrogen and sulfur (78).

The two-layer MLP model's permutation feature importance method was used to evaluate the impact of different input factors on uranium adsorption capacity. Figure 5 shows that, of the chemical properties of biochar, carbon content was the second most important factor influencing uranium adsorption (73). Additionally, within the 20–50% range, there was a negative correlation between the adsorption capacity and the mass percentage of total carbon (C, wt%). The correlation steadily stabilized outside of this range. According to Zhu et al. (75), the carbon content contributed 10% to the properties of biochars, underscoring the importance of carbon content for the adsorption of heavy metals (Figure 5).

According to Jaffari et al. (79), biochar materials have recently drawn a lot of interest as economical and environmentally friendly adsorbents because of their capacity to effectively remove dangerous new contaminants (like fungicides, herbicides, and pharmaceuticals) that endanger aquatic life and human health in aquatic ecosystems. Ten tree-based machine learning models were created as part of their study with the goal of precisely forecasting



the ability of biochar materials to adsorb emerging contaminants (ECs) from water. With the highest test coefficient of determination (0.9433) and the lowest mean absolute error (4.95 mg/g), the CatBoost model outperformed all other models in the ML model evaluations. The Shapley Additive Explanations (SHAP) analysis revealed that the adsorbent composition, which included N/C, C%, H/C, O/C, (O+N)/C, and ash, significantly influenced (35%) model predictions for the adsorption capacity of fungicides, pharmaceuticals, and herbicides.

6.2 Aromatization degree of biochar

The H/C and O/C ratios of biochar act as markers of its carbonization, aromaticity, and maturity levels. The substantial amount of C in biochar indicates the predominance of aromatic structure following carbonization. Reduced ratios indicate a more complete dehydration process and significant aromatic condensation during biomass (80) pyrolyzed. Comparably, the O/C ratio shows the surface hydrophilicity of biochar; a high ratio denotes great surface hydrophilicity (81). These H/C and O/C ratios typically drop with increasing pyrolysis temperature, indicating increased aromaticity and stability, lowered polarity, and hence, more hydrophobicity. Low H/C and O/C ratios also confirm more consistent biochar; an O/C ratio less than 0.2 indicates great stability (82). The atomic ratios of O/C, H/C, and (O + N)/C are calculated to evaluate aromaticity, polarity, and longevity of biochar (83). Using PCC and SHAP analyses, Song et al. (84) investigated the main relationships in biochar between ten input variables and the H/C, N/C, and O/C ratios. With a PCC=-0.8 the results showed a strong negative correlation between the H/C and O/C ratios of biochar and temperature. Other factors showing PCC values \leq 0.2, implying a rather small influence were VM, FC, and AC. Supported by SHAP value analysis, these findings revealed that the H/C and O/C ratios depend critically on pyrolyzed temperature. Rising pyrolysis temperature reduces the H/C and O/C ratios, so indicating enhanced aromaticity in the biochar. Higher pyrolysis temperatures thus improve biochar aromaticity, most likely due to increased dehydration, decarboxylation, and demethylation reactions in the biomass at higher temperatures, so producing more complete biochar development reactions (85, 86). On the other hand, the N/C ratio of biochar had a rather strong positive correlation with temperature. The SHAP value analysis confirmed this link even more by stressing pyrolysis temperature as a main determinant of the N/C ratio. The N/ C ratio likewise rises as the pyrolyze temperature rises. Mostly derived from proteins, N in biomass changes during pyrolysis into gaseous, liquid, and solid forms. N mostly exists in biochar as N-C and N-H bonds with low migration potential. About thirty percent of N stays in the biochar even at 900°C, the pyrolyze temperature. Considering the conservation of C, H, O, and N elements in biochar, the rise in the N/C ratio with higher pyrolysis temperatures results from the nitrogen's resistance to migration.

The H/C and (O + N)/C molar ratios explained an 11% involvement to the properties of biochars in the research carried out by Zhu et al. (75), so emphasizing the relevance of oxygen-

containing functional groups and aromatic structures in the adsorption process of heavy metals (Figure 5). This implies that the presence of these functional groups increases the capacity of the biochar to interact with and bind heavy metal ions, so improving its adsorbent efficiency. The interaction of these ratios suggests that the adsorption capacity of biochar depends critically on both its structural and chemical composition. A multilayer perceptron artificial neural network (MLP ANN) model (R² ≈ 0.99, RMSE = 3.75) outperformed support vector regression (SVR), random forest (RF), and linear regression models in predicting uranium adsorption capacity on biochar, Da et al. (73). They also discovered that changing the structural characteristics of biochar, especially the oxygen-tocarbon (O/C) ratio, might increase its adsorbing capacity for radioactive uranium. Their data indicate that the most important chemical feature influencing uranium adsorption is the O/C ratio. Research already in publication supports that raising the O/C ratio and building the micro- and mesoporous structure of biochar will greatly increase its uranium adsorption capacity (87). Furthermore shown by a positive correlation between uranium adsorption capacity and the O/C ratio was the importance of oxygen-containing functional groups in improving adsorption.

These revelations can be used to design and engineer biochar with ideal characteristics for maximum contaminant removal from soil and water, so offering a useful approach for environmental remedial projects.

6.3 Cation exchange capacity

Biochar's cation exchange capacity is the ability of it to help cations in solution to migrate. Cation exchange capacity (17) is notably and favorably correlated with functional groups including O/C and (O+N)/C, which provide active sites for cation exchange with heavy metals). This correlation has been established as one of the principal adsorption mechanisms facilitating the removal of heavy metals (Cd, Cu, Pb etc.) from aqueous solutions. Consequently, cation exchange capacity ranked second feature in importance, following heavy metal adsorption capacity (17). Furthermore, predicting biochar's properties, such as cation exchange capacity, leads to realizing the down-to-earth application of biochar for adsorbing contaminants. Therefore, Shen et al. (17) utilized biomass based on agricultural and forestry wastes, sewage sludge, and algae and predicted the cation exchange capacity using GBR and RF. The authors applied supervised ML models (GBR model: train; R² = 0.94, RMSE = 2.14; test; $R^2 = 0.74$, RMSE = 3.44, whereas RF model: train; $R^2 =$ 0.80, RMSE = 4.27; test; $R^2 = 0.82$, RMSE = 2.39) to optimize the biochar cation exchange capacity in biomass pyrolysis using 353 data points with 80% training and 20% testing data. Results indicated that the GBR performed better than the RF.

Using ML approaches, Zhu et al. (75) modeled the adsorption behavior of six heavy metals—Pb, Cd, Ni, As, Cu, and Zn)—on 44 different kinds of biochar. Using a dataset totaling 353 adsorption studies, they especially used ANN and RF models. With a R² value of 0.973 rather than 0.948 for the ANN, their findings showed that the

RF model outperformed the ANN model with a greater accuracy. With 54% of the observed variation taken into account, the study revealed that CEC turned out as one of the most important biochar properties in determining adsorption efficiency (Figure 5). This emphasizes the important part CEC plays in the adsorption process since it influences the general chemical interactions between the metal ions and biochar as well as cation retention. The type of surface functional groups and the mineral composition of the biochars determine the great correlation between CEC and adsorption efficiency. Furthermore connected to the higher contributions of CEC could be the presence of ion-exchange contents (such as K⁺, Na⁺, Ca²⁺, and Mg²⁺) and different surface functional groups (88). These elements improve the CEC, hence biochars with higher CEC are more efficient in heavy metal adsorbing. The results of their research imply that maximizing the CEC of biochars could be a main focus for enhancing their performance as adsorbents in applications related to water and wastewater treatment.

6.4 Electrical conductivity

Although biochar is clearly important for energy generation, conversion, and storage—mostly because of its remarkable electrical conductivity—there is still a dearth of predictive research on this fundamental characteristic. Because of its unique properties including electrical conductivity, which makes it appropriate for many uses including Li/Na ion batteries, supercapacitors, H2 storage, and O2 electro-catalysis, biochar plays a key role in energy production, conversion and storage (89, 90). The literature regarding the prediction of biochar's electrical conductivity is scarce therefore, first time Abdi et al. (44) predicted the electrical conductivity of compost (Cooked rice, coco peat, residues of vegetables such as cabbage, squash, lettuce) with biochar additive in in-vessel composting machine by ANN and ANFIS. The statistical results of ANN and ANFIS models for predicting electrical conductivity revealed that ANFIS provided more accurate prediction than ANN with highest R² value (0.999) and the lowest value of RMSE (0.002) (Table 1). However, this represents an initial foray rather than a comprehensive understanding. Critical gaps persist in elucidating the electron transfer pathways within biochar matrices, particularly regarding the influence of feedstock type, pyrolysis conditions, and surface chemistry. Future research should prioritize mechanistic studies integrating advanced spectroscopic techniques and computational modeling to unravel these processes. Furthermore, extending predictive modeling efforts over several biochar varieties and functionalization techniques will hasten the customized design of biochars best fit for particular electrochemical uses.

6.5 Capacitance

Advancement of renewable energy depends most on biochar, a novel kind of energy storage acting as a supercapacitor (91). The energy storing capacity of supercapacitors is mostly determined by

the electrode material. In this sense, the carbon-based raw material shows to be the ideal precursor because of its cheap character and great conductivity (92). Biochar-based electrode materials derived from biomass resources have rather strong capacitance storage properties (93). ML is essential in producing predictions using biochar-related input parameters if one wants to maximize the capacitance of electrodes based on biochar for supercapacitors. In this regard, Wickramaarachchi et al. (55) carbonized carbon and subsequently chemically activated it with KOH using biowaste comprising mango seed fiber to produce sustainable supercapacitor material. Furthermore projected using ML models including DT, MLP, and SVR was the energy storage performance of the produced activated carbon samples. These models made use of input parameters comprising biochar physical conditions (specific surface area, pore volume, average pore diameter, and current density), activation conditions (activation time, activation temperature), and specific surface area. With its maximum R² value (0.99) and lowest RMSE value (4.1), the statistical analysis of several machine learning models used to forecast capacitance showed that MLP produced a more accurate prediction than DT and SVR. Table 1 lists more research on ML techniques for biochar capacitance prediction.

6.6 Functional groups

Surface properties of biochar, such N-containing functional groups (94), which offer active sites for heavy metal adsorption via covalent solid bonding, chelation, electrostatic attraction, and hydrogen bonding (95) define its performance in terms of contaminant adsorption. Regarding the relevance of functional groups in biochar studies, Palansooriya et al. (96) said that the N-containing functional group in biochar ranked first among twenty variables including a specific surface area that considerably influences the immobilization of heavy metal by biochar in soil. Leng et al. (52) thus projected and optimized the N content of biochar made from corn husk, rice husk, and sawdust using machine learning models and showed GBR outperformed RF with the maximum train R2 value (0.90) and the lowest train RMSE value (0.38).

Zhu et al. (97) designed two ML models with varying material property emphasis. Along with reaction conditions including solution pH (pHsol), temperature (T), and initial concentration (C0), the first model—Model BP—used basic properties (BP) of biochar (BC) and iron-impregnated biochar (Fe-BC), including carbon content (C), oxygen-to—carbon ratio (O/C), iron content (Fe), and specific surface area (SBET). By contrast, the second model, Model SF, included non-polar carbon (NPC), C-O, and C=O groups instead of just C and O/C by including detailed surface functionalities (SF) of BC and Fe-BC. With a R² of 0.889 and an RMSE of 13.8 mg/g in the test group, the results showed that Model BP based on fundamental surface properties and reaction conditions could forecast the removal capacity for aqueous chromium (VI) (Cr(VI)). This good predictive performance shows how well surface chemical information obtained from XPS

data is used. Moreover, the predictive accuracy was much enhanced by including relative proportions of surface functional groups into Model SF, so stressing the important part these groups play in predicting the removal capacity of BC and Fe-BC for Cr(VI).

Since oxygen-containing groups such C-O and C=O on the biochar surface help to both reduce and adsorption of Cr(VI), the O/C ratio was found in Model BP to be the most important element influencing Cr(VI) removal capacity. The effect of iron impregnation on the relative proportions of C-O and C=O was also investigated; in Model SF C-O had a greater relative importance than C=O. Supported by the recorded consumption of C-O groups in biochar following Cr(VI) removal, the presence of C-O groups acts as electron donors, so helping to reduce Cr(VI) to Cr(III). As electron donors, functional groups including C-OH, -COOH, and -OH significantly help to lower Cr(VI) to Cr(III) (98). Furthermore noted to help lower Cr(VI) to Cr(III) were oxygenbased functional groups including C-OH (99). Redox cycles formed by C-O groups in Fe-BC couple with C=O or iron species to further reduce Cr(VI). Nevertheless, the ideal ratio of C-O (i.e., from ~ 29% to ~ 38%) for the effective elimination of aqueous Cr(VI) has yet to be exactly determined; hence, more experimental and theoretical study is needed to validate these conclusions (100).

The greater significance of C-O compared to C=O in biochar for removing Cr(VI), can be attributed to its higher reduction potential (101). The impact of C-O and C=O on Cr(VI) removal capacity varies. The partial dependence plot (PDP) for C=O illustrates a direct increase in Cr(VI) removal efficiency as the C=O content rises until it reaches about 25%, after which the removal efficiency declines. In acidic conditions, carbonyl or carboxylic groups (C=O) can be protonated, enabling them to either electrostatically attract the negatively charged Cr(VI) species or interact with oxygen in $HCrO_4$ - and $Cr_2O_7^{2-}$ through hydrogen bonding (102). However, the electron-deficient nature of C=O groups makes them more likely to accept electrons, potentially diminishing the biochar's redox reaction efficiency for converting Cr(VI) to Cr(III) and reducing its Cr(VI) removal capacity (103). The reduction of Cr(VI) is primarily attributed to reductive moieties in biochar, with oxygencontaining functional groups such as -OH and COC serving as relatively weak electron donors in neutral and alkaline conditions (103). However, stronger electron donors, such as persistent free radicals (PFRs) detected in biochar, are hypothesized to be associated with the favorable reduction of Cr(VI) (103).

Particularly for ECs, the SHAP analysis in Jaffari et al. (79) underlines the major impact of the nitrogen-to- carbon (N/C) ratio on the adsorption performance of biochar. On the biochar surface, nitrogen-containing functional groups including amines (-NH₂), imines (=NH), and other -NHx species are absolutely important for contaminant binding. By means of both covalent and ionic interactions with pollutants, these groups improve adsorption efficiency. Often via electron sharing or donor-acceptor mechanisms, covalent bonding results from nitrogen groups forming strong chemical bonds with reactive functional groups on contaminants. Stable complexes can be produced, for instance, by lone pair electrons on nitrogen atoms interacting with electrophilic sites on organic molecules or heavy metals. By electrostatic forces,

protonated nitrogen groups (-NH₃⁺) draw negatively charged pollutants, so facilitating adsorption through charge complementarity. Different functional groups on the surface of biochar enhance its reactivity and affinity for different pollutants, so enabling more successful binding of pollutants (104). Higher adsorption capacity does not always match, though, an increasing N/C ratio. At quite high nitrogen contents, the expected adsorption capacity falls. This could be the result of competitive effects whereby too nitrogen-containing groups—from hydrolysis of proteins and nucleic acids or synthesis of nitrogen-homogeneous compounds during pyrolysis (105)—form a hydrophilic water film barrier on the biochar surface. This barrier limits adsorption by blocking access to internal pores and active sites. Furthermore, highly packed nitrogen groups might change surface chemistry negatively or fight for binding sites.

Richer datasets for future ML models will help them to better differentiate among nitrogen functional groups and clarify their different binding mechanisms. Maximizing the adsorption capacity and specificity of biochar by optimizing the balance and types of nitrogen groups together with building suitable porosity and surface functionalities will help to improve its environmental remedial capacity.

7 Improving model interpretability by cooperative interdisciplinary work

Many times involving intricate algorithms that might limit interpretability, ML models applied in biochar design can impede useful implementation. This gap can be closed with cooperative frameworks that aggressively involve environmental scientists in tandem with data scientists. Environmental experts provide important new perspectives on biochar processes, contaminant behavior, and system dynamics so facilitating more significant interpretation of model outputs. Such collaborations can take the form of iterative processes whereby co-management of model development, validation, and interpretation guarantees models are both operationally relevant and scientifically strong. Standardizing data sharing, model explanations, and cross-disciplinary communication will help to improve these initiatives even more. Emphasizing these partnerships not only increases model transparency but also helps stakeholders to build trust, so accelerating the application of ML-optimized biochar technologies in practical environmental remediation.

8 Conclusion and future perspective

This review evaluates the strengths and constraints of present methods as well as the transforming possibilities of ML in advancing engineered biochar for contaminant remediation. By means of analysis of complicated interactions between feedstock composition, pyrolysis conditions, and activation techniques, the strong evidence in the literature shows that ML can efficiently

maximize biochar properties—such as surface area, pore structure, and functional groups. Particularly ensemble and deep learning methods, ML models have shown great ability to lower experimental trial-and-error, so accelerating the design of high-performance biochars for intended pollution reduction.

Important flaws still exist in the field, though. Although ML glows in predictive modeling and pattern recognition, it sometimes lacks mechanical interpretability, which makes it challenging to fully understand why particular biochar modifications produce better adsorption. Many studies also depend on small or inconsistent datasets, so restricting model generalizability under different environmental conditions. Furthermore, dynamic realworld events like changing water chemistry or long-term biochar aging—which greatly affect remedial efficacy—are not easily explained by ML by itself.

Overcoming these constraints requires hybrid methods combining basic science with ML. Combining molecular-scale simulations (e.g., DFT) with ML could clarify atomic-level interactions between biochar surfaces and contaminants, so bridging the gap between data-driven predictions and mechanistic knowledge. By tying expected performance to observable chemical changes, pairing ML with advanced spectroscopy—e.g., *in situ* FTIR, XPS—may help to validate model outputs. Furthermore, including kinetic and thermodynamic ideas into ML models might improve their field-scale applicability and time-dependent adsorption behavior prediction capability.

There is still a great knowledge vacuum about how biochar features affect microbial populations that help to degrade pollutants. Future research should give ML models including microbiological data top priority in order to maximize biochar for sustaining beneficial microbial activity as well as for adsorption. Ultimately, even if ML-driven biochar generation shows potential to lower carbon emissions, its actual environmental impact has to be carefully evaluated using life-cycle studies included into modeling processes.

Through multidisciplinary collaboration—merging ML with chemistry, microbiology, and environmental engineering—the next generation of biochar design can achieve both precision and sustainability, so releasing its full potential for worldwide remediation activities.

Author contributions

YG: Writing – original draft, Data curation, Conceptualization, Methodology. KY: Software, Data curation, Writing – review &

editing. GY: Investigation, Formal analysis, Resources, Writing – review & editing. MA: Project administration, Writing – review & editing. AI: Funding acquisition, Resources, Writing – review & editing. AS: Investigation, Software, Writing – review & editing, Formal analysis. HU: Investigation, Supervision, Writing – review & editing, Writing – original draft, Formal analysis.

Funding

The author(s) declare that financial support was received for the research and/or publication of this article. The current work was supported by the Guangxi Science and Technology Project (2025) GXNSFAA069282, and Guangxi Technology Base and Talent Subject (GUIKE AD23023008). The authors extend their appreciation to the Deanship of Research and Graduate Studies at King Khalid University for funding this work through Large Research Project under grant number RGP2/475/46.

Conflict of interest

The authors declare that the research was conducted in the absence of any commercial or financial relationships that could be construed as a potential conflict of interest.

Correction note

A correction has been made to this article. Details can be found at: 10.3389/fsoil.2025.1659154.

Generative Al statement

The author(s) declare that no Generative AI was used in the creation of this manuscript.

Publisher's note

All claims expressed in this article are solely those of the authors and do not necessarily represent those of their affiliated organizations, or those of the publisher, the editors and the reviewers. Any product that may be evaluated in this article, or claim that may be made by its manufacturer, is not guaranteed or endorsed by the publisher.

References

- 1. Aggelopoulos CA. Recent advances of cold plasma technology for water and soil remediation: A critical review. *Chem Eng J.* (2022) 428:131657. doi: 10.1016/j.cej.2021.131657
- 2. El-Sharkawy M, Li J, Kamal N, Mahmoud E, Omara AED, Du D. Assessing and predicting soil quality in heavy metal-contaminated soils: statistical and ANN-based techniques. J Soil Sci Plant Nutr. (2023) 23:6510–26. doi: 10.1007/s42729-023-01507-w
- 3. Nnabuchi MA, Duru CD. Computational and theoretical approach to deciphering potential PFAS-induced toxicity on the human estrogen and sperm receptors, with implications on female fertility. *Medinformatics*. (2025) 2(2):132–44. doi: 10.47852/bonviewMEDIN52024770
- 4. Vishnoi S, Goel RK. Climate smart agriculture for sustainable productivity and healthy landscapes. *Environ Sci Policy*. (2024) 151:103600. doi: 10.1016/j.envsci.2023.103600

- 5. Anjum M, Siddique N, Younis H, Faiz Y, Shafique MA, Mahnoor A, et al. Heavy metals and radionuclides in Islamabad's industrial area: A comprehensive analysis of soil and water pollution, source apportionment and health effects using statistical and geospatial tools. *J Trace Elem Miner*. (2024) 8:100127. doi: 10.1016/j.jtemin.2024.100127
- 6. UNEP. Information on the implementation of resolution 3/10 on addressing water pollution to protect and restore water-related ecosystems (UNEP/EA.6/INF/4). (2023) Nairobi: United Nations Environment Assembly.
- 7. Sharma P. Biochar colloids mobilization by consecutive fluid displacement in unsaturated condition. *Groundw Sustain Dev.* (2023) 23:101030. doi: 10.1016/j.gsd.2023.101030
- 8. Zhou Y, Leong SY, Li Q. Modified biochar for removal of antibiotics and antibiotic resistance genes in the aqueous environment: A review. *J Water Process Eng.* (2023) 55:104222. doi: 10.1016/j.jwpe.2023.104222
- 9. Jing Y, Zhang Y, Han I, Wang P, Mei Q, Huang Y. Effects of different straw biochars on soil organic carbon, nitrogen, available phosphorus, and enzyme activity in paddy soil. *Sci Rep.* (2020) 10:8837. doi: 10.1038/s41598-020-65796-2
- 10. Fan X, Peng L, Wang X, Han S, Yang L, Wang H, et al. Efficient capture of lead ion and methylene blue by functionalized biomass carbon-based adsorbent for wastewater treatment. *Ind Crops Prod.* (2022) 183:114966. doi: 10.1016/j.indcrop.2022.114966
- 11. Girkar M, Shukla SP, Bharti V, Kumar K, Kumar S, Rathi Bhuvaneswari G. Removal of fluoride from groundwater by chemically functionalized sugarcane bagasse biochar and bagasse pellets in a fixed-bed sorption system. *Desalin Water Treat.* (2024) 317:100044. doi: 10.1016/j.dwt.2024.100044
- 12. Ullah H, Khan S, Zhu X, Chen B, Rao Z, Wu N, et al. Machine learning-aided biochar design for the adsorptive removal of emerging inorganic pollutants in water. *Sep Purif Technol.* (2025) 362:131421. doi: 10.1016/j.seppur.2025.131421
- 13. Zhang P, Zhang T, Zhang J, Liu H, Chicaiza-Ortiz C, Lee JTE, et al. A machine learning assisted prediction of potential biochar and its applications in anaerobic digestion for valuable chemicals and energy recovery from organic waste. *Carbon Neutrality*. (2024) 3:5. doi: 10.1007/s43979-023-00078-0
- 14. Jeyaraj SG, Hemavarshini S, Shree KGG, Aravind J. Biochar-mediated removal of various pollutants from the environment. *Phys Sci Rev.* (2024) 9:3409–31. doi: 10.1515/psr-2023-0043
- 15. Kapoor RT, Zdarta J. Fabrication of engineered biochar for remediation of toxic contaminants in soil matrices and soil valorization. *Chemosphere.* (2024) 358:142101. doi: 10.1016/j.chemosphere.2024.142101
- 16. Chen MW, Chang MS, Mao Y, Hu S, Kung CC. Machine learning in the evaluation and prediction models of biochar application: A review. *Sci Prog.* (2023) 106:368504221148842. doi: 10.1177/00368504221148842
- 17. Shen T, Peng H, Yuan X, Liang Y, Liu S, Wu Z, et al. Feature engineering for improved machine-learning-aided studying heavy metal adsorption on biochar. *J Hazard Mater*. (2024) 466:133442. doi: 10.1016/j.jhazmat.2024.133442
- 18. Leng L, Lei X, Abdullah Al-Dhabi N, Wu Z, Yang Z, Li T, et al. Machine-learning-aided prediction and engineering of nitrogen-containing functional groups of biochar derived from biomass pyrolysis. *Chem Eng J.* (2024) 485:149862. doi: 10.1016/j.cej.2024.149862
- 19. Li H, Ai Z, Yang L, Zhang W, Yang Z, Peng H, et al. Machine learning assisted predicting and engineering specific surface area and total pore volume of biochar. *Bioresour Technol.* (2023) 369:128417. doi: 10.1016/j.biortech.2022.128417
- 20. Wang W, Chang J-S, Lee D-J. Machine learning applications for biochar studies: A mini-review. *Bioresour Technol*. (2024) 394:130291. doi: 10.1016/j.biortech.2023.130291
- 21. Zhang J, Chen Z, Liu Y, Wei W, Ni B-J. Removal of emerging contaminants (ECs) from aqueous solutions by modified biochar: A review. *Chem Eng J.* (2024) 479:147615. doi: 10.1016/j.cej.2023.147615
- 22. El-Naggar A, Ahmed N, Mosa A, Niazi NK, Yousaf B, Sharma A, et al. Nickel in soil and water: Sources, biogeochemistry, and remediation using biochar. *J Hazard Mater*. (2021) 419:126421. doi: 10.1016/j.jhazmat.2021.126421
- 23. Qiu M, Liu L, Ling Q, Cai Y, Yu S, Wang S, et al. Biochar for the removal of contaminants from soil and water: a review. *Biochar*. (2022) 4:19. doi: 10.1007/s42773-022-00146-1
- 24. Nie J, Zhi D, Zhou Y. Chapter 8 Magnetic biochar-based composites for removal of recalcitrant pollutants in water. In: Núñez-Delgado A, editor. Sorbents Materials for Controlling Environmental Pollution. Elsevier (2021). p. 163–87.
- 25. Yang M. Performance and mechanism of Cr(VI) removal by sludge-based biochar loaded with zero-valent iron. Desalin Water Treat. (2024) 317:100035. doi: 10.1016/j.dwt.2024.100035
- 26. Junfeng W, Bowen H, Xiaoqing W, Zuwen L, Zhaodong W, Biao L, et al. Preparation of N,S-codoped magnetic bagasse biochar and adsorption characteristics for tetracycline. *RSC Adv.* (2022) 12:11786–95. doi: 10.1039/d1ra08404f
- 27. Wang Q, Zhang Z, Xu G, Li G. Pyrolysis of penicillin fermentation residue and sludge to produce biochar: Antibiotic resistance genes destruction and biochar application in the adsorption of penicillin in water. *J Hazard Mater.* (2021) 413:125385. doi: 10.1016/j.jhazmat.2021.125385
- 28. Ali SM, El Mansop MA, Galal A, Abd El Wahab SM, El-Etr WMT, Zein El-Abdeen HA. A correlation of the adsorption capacity of perovskite/biochar composite

with the metal ion characteristics. Sci Rep. (2023) 13:9466. doi: 10.1038/s41598-023-36592-5

- 29. Chanda RK, Jahid T, Hassan MN, Yeasmin T, Biswas BK. Cauliflower stemderived biochar for effective adsorption and reduction of hexavalent chromium in synthetic wastewater: A sustainable approach. *Environ Adv.* (2024) 15:100458. doi: 10.1016/j.envadv.2023.100458
- 30. Li N, Liu Y, Du C, Wang Y, Wang L, Li X. A novel role of various hydrogen bonds in adsorption, desorption and co-adsorption of PPCPs on corn straw-derived biochars. *Sci Total Environ*. (2023) 861:160623. doi: 10.1016/j.scitotenv.2022.160623
- 31. Ambaye TG, Vaccari M, van Hullebusch ED, Amrane A, Rtimi S. Mechanisms and adsorption capacities of biochar for the removal of organic and inorganic pollutants from industrial wastewater. *Int J Environ Sci Technol.* (2021) 18:3273–94. doi: 10.1007/s13762-020-03060-w
- 32. Puga A, Moreira MM, Pazos M, Figueiredo SA, Sanromán MÁ, Delerue-Matos C, et al. Continuous adsorption studies of pharmaceuticals in multicomponent mixtures by agroforestry biochar. *J Environ Chem Eng.* (2022) 10:106977. doi: 10.1016/j.jece.2021.106977
- 33. Liu L, Fan S, Wang Z, Hu J. Chemical speciation distribution, desorption characteristics, and quantitative adsorption mechanisms of cadmium/lead ions adsorbed on biochars. *Arab J Chem.* (2024) 17:105669. doi: 10.1016/j.arabjc.2024.105669
- 34. Bibi A, Ur Rahman JS. Machine learning enabled in-home ECG: A review. *Medinformatics.* (2025). doi: 10.47852/bonviewMEDIN52024336
- 35. Ascher S, Watson I, You S. Machine learning methods for modelling the gasification and pyrolysis of biomass and waste. *Renew Sustain Energy Rev.* (2022) 155:111902. doi: 10.1016/j.rser.2021.111902
- 36. Hassija V, Chamola V, Mahapatra A, Singal A, Goel D, Huang K, et al. Interpreting black-box models: A review on explainable artificial intelligence. *Cogn Comput.* (2024) 16:45–74. doi: 10.1007/s12559-023-10179-8
- 37. Rajula HSR, Verlato G, Manchia M, Antonucci N, Fanos V. Comparison of conventional statistical methods with machine learning in medicine: diagnosis, drug development, and treatment. *Medicina*. (2020) 56:455. doi: 10.3390/medicina56090455
- 38. Morales EF, Escalante HJ. Chapter 6 A brief introduction to supervised, unsupervised, and reinforcement learning. In: Torres-García AA, Reyes-García CA, Villaseñor-Pineda L, Mendoza-Montoya O, editors. Biosignal Processing and Classification Using Computational Learning and Intelligence. Academic Press (2022). p. 111–29.
- 39. Tran HQ, Ha C. Machine learning in indoor visible light positioning systems: A review. *Neurocomputing*. (2022) 491:117–31. doi: 10.1016/j.neucom.2021.10.123
- 40. Chang X, Huang X, Xu W, Tian X, Wang C, Wang L, et al. Monitoring of dough fermentation during Chinese steamed bread processing by near-infrared spectroscopy combined with spectra selection and supervised learning algorithm. *J Food Process Eng.* (2021) 44:e13783. doi: 10.1111/jfpe.13783
- 41. Eppe M, Gumbsch C, Kerzel M, Nguyen PDH, Butz MV, Wermter S. Intelligent problem-solving as integrated hierarchical reinforcement learning. *Nat Mach Intell.* (2022) 4:11–20. doi: 10.1038/s42256-021-00433-9
- 42. Adeyanju SA, Ogunjobi TT. Machine learning in genomics: applications in whole genome sequencing, whole exome sequencing, single-cell genomics, and spatial transcriptomics. *Medinformatics*. (2024). doi: 10.47852/bonviewMEDIN42024120
- 43. Wang H, Gu J, Wang M. A review on the application of computer vision and machine learning in the tea industry. *Front Sustain Food Syst.* (2023) 7:1172543. doi: 10.3389/fsufs.2023.1172543
- 44. Abdi R, Shahgholi G, Sharabiani VR, Fanaei AR, Szymanek M. Prediction of compost criteria of organic wastes with biochar additive in in-vessel composting machine using ANFIS and ANN methods. *Energy Rep.* (2023) 9:1684–95. doi: 10.1016/j.egyr.2023.01.001
- 45. Hai A, Bharath G, Patah MFA, Daud WMAW, Rambabu K, Show P, et al. Machine learning models for the prediction of total yield and specific surface area of biochar derived from agricultural biomass by pyrolysis. *Environ Technol Innov.* (2023) 30:103071. doi: 10.1016/j.eti.2023.103071
- 46. Henseler J, Ringle C, Sinkovics R. The use of partial least squares path modeling in international marketing. Adv Int Mark. (2009) 20:277–319. doi: 10.1108/S1474-7979 (2009)000020014
- 47. Li X, Su J, Wang H, Boczkaj G, Mahlknecht J, Singh S, et al. Bibliometric analysis of artificial intelligence in wastewater treatment: Current status, research progress, and future prospects. *J Environ Chem Eng.* (2024) 12:113152. doi: 10.1016/j.jece.2024.113152
- 48. Oral B, Coşgun A, Günay ME, Yıldırım R. Machine learning-based exploration of biochar for environmental management and remediation. *J Environ Manage*. (2024) 360:121162. doi: 10.1016/j.jenvman.2024.121162
- 49. Yuan X, Cao Y, Li J, Patel AK, Dong CD, Jin X, et al. Recent advancements and challenges in emerging applications of biochar-based catalysts. *Biotechnol Adv.* (2023) 67:108181. doi: 10.1016/j.bioteChadv.2023.108181
- 50. Zhao F, Tang L, Song W, Jiang H, Liu Y, Chen H. Predicting and refining acid modifications of biochar based on machine learning and bibliometric analysis: Specific surface area, average pore size, and total pore volume. *Sci Total Environ.* (2024) 948:174584. doi: 10.1016/j.scitotenv.2024.174584
- 51. Yargicoglu EN, Sadasivam BY, Reddy KR, Spokas K. Physical and chemical characterization of waste wood derived biochars. *Waste Manage*. (2015) 36:256–68. doi: 10.1016/j.wasman.2014.10.029

- 52. Leng L, Yang L, Lei X, Zhang W, Ai Z, Yang Z, et al. Machine learning predicting and engineering the yield, N content, and specific surface area of biochar derived from pyrolysis of biomass. *Biochar.* (2022) 4:63. doi: 10.1007/s42773-022-00183-w
- 53. Li X, Huang Z, Shao S, Cai Y. Machine learning prediction of physical properties and nitrogen content of porous carbon from agricultural wastes: Effects of activation and doping process. *Fuel.* (2024) 356:129623. doi: 10.1016/j.fuel.2023.129623
- 54. Zhou X, Liu X, Sun L, Jia X, Tian F, Liu Y, et al. Prediction of biochar yield and specific surface area based on integrated learning algorithm. *Journal of Carbon Research*. (2024) 10(1):10. doi: 10.3390/c10010010
- 55. Wickramaarachchi WAMKP, Minakshi M, Gao X, Dabare R, Wong KW. Hierarchical porous carbon from mango seed husk for electro-chemical energy storage. *Chem Eng J Adv.* (2021) 8:100158. doi: 10.1016/j.ceja.2021.100158
- 56. Yang X, Yuan C, He S, Jiang D, Cao B, Wang S. Machine learning prediction of specific capacitance in biomass derived carbon materials: Effects of activation and biochar characteristics. *Fuel.* (2023) 331:125718. doi: 10.1016/j.fuel.2022.125718
- 57. Sun Y, Sun P, Jia J, Liu Z, Huo L, Zhao L, et al. Machine learning in clarifying complex relationships: Biochar preparation procedures and capacitance characteristics. *Chem Eng J.* (2024) 485:149975. doi: 10.1016/j.cej.2024.149975
- 58. Guo S, Li Y, Wang Y, Wang L, Sun Y, Liu L. Recent advances in biochar-based adsorbents for CO2 capture. *Carbon Capture Sci Technol.* (2022) 4:100059. doi: 10.1016/j.ccst.2022.100059
- 59. Yaashikaa PR, Kumar PS, Varjani S, Saravanan A. A critical review on the biochar production techniques, characterization, stability and applications for circular bioeconomy. *Biotechnol Rep.* (2020) 28:e00570. doi: 10.1016/j.btre.2020.e00570
- 60. Liang L, Xi F, Tan W, Meng X, Hu B, Wang X. Review of organic and inorganic pollutants removal by biochar and biochar-based composites. *Biochar*. (2021) 3:255–81. doi: 10.1007/s42773-021-00101-6
- 61. Qiu L, Li C, Zhang S, Wang S, Li B, Cui Z, et al. Distinct property of biochar from pyrolysis of poplar wood, bark, and leaves of the same origin. *Ind Crops Prod.* (2023) 202:117001. doi: 10.1016/j.indcrop.2023.117001
- 62. Yang Z, Hou J, Wu J, Miao L. The effect of carbonization temperature on the capacity and mechanisms of Pb(II) adsorption by microalgae residue-derived biochar. *Ecotoxicol Environ Saf.* (2021) 225:112750. doi: 10.1016/j.ecoenv.2021.112750
- 63. Liu Z, Zhang P, Wei Z, Xiao F, Liu S, Guo H, et al. Porous Fe-doped graphitized biochar: An innovative approach for co-removing per-/polyfluoroalkyl substances with different chain lengths from natural waters and wastewater. *Chem Eng J.* (2023) 476:146888. doi: 10.1016/j.cej.2023.146888
- 64. Mustapha LS, Obayomi OV, Yahya MD, Lau SY, Obayomi KS. Exploring the synergistic effects of calcium chloride modification on stem bark eucalyptus biochar for Cr(VI) and Pb(II) ions removal: Kinetics, isotherm, thermodynamic and optimization studies. *Bioresour Technol Rep.* (2024) 25:101699. doi: 10.1016/j.biteb.2023.101699
- 65. Ilyas M, Liao Y, Xu J, Wu S, Liao W, Zhao X. Removal of anthracene from vehicle-wash wastewater through adsorption using eucalyptus wood waste-derived biochar. *Desalin Water Treat*. (2024) 317:100115. doi: 10.1016/j.dwt.2024.100115
- 66. Varela CF, Moreno-Aldana LC, Agámez-Pertuz YY. Adsorption of pharmaceutical pollutants on ZnCl2-activated biochar from corn cob: Efficiency, selectivity and mechanism. *J Bioresour Bioprod.* (2024) 9:58–73. doi: 10.1016/j.jobab.2023.10.003
- 67. Vinayagam R, Nagendran V, Goveas LC, Narasimhan NK, Varadavenkatesan T, Samanth A, et al. "Machine Learning. Conventional and Statistical Physics Modeling of 2,4-Dichlorophenoxyacetic Acid (2,4-D) Herbicide Removal Using Biochar Prepared from Vateria Indica Fruit Biomass." *Chemosphere.* (2024) 350:141130. doi: 10.1016/j.jhazmat.2019.06.004
- 68. Lu X, Zhao J. Adsorption of ciprofloxacin on co-pyrolyzed biochar from fish scale and pine needle. *Chin J Anal Chem.* (2024) 52:100350. doi: 10.1016/j.cjac.2023.100350
- 69. Wang X, Wang T, Huang Y, Liu A, Li Q, Wang Y, et al. Effect of biochars on the immobilization and form of Cadmium (Cd) in simulated Cd deposition of iron rich soils. *Ecotoxicol Environ Saf.* (2024) 272:116045. doi: 10.1016/j.ecoenv.2024.116045
- 70. Tomin O, Vahala R, Yazdani MR. Synthesis and efficiency comparison of reed straw-based biochar as a mesoporous adsorbent for ionic dyes removal. *Heliyon*. (2024) 10:e24722. doi: 10.1016/j.heliyon.2024.e24722
- 71. Tcheka C, Conradie MM, Assinale VA, Conradie J. Mesoporous biochar derived from Egyptian doum palm (Hyphaene thebaica) shells as low-cost and biodegradable adsorbent for the removal of methyl orange dye: Characterization, kinetic and adsorption mechanism. *Chem Phys Impact.* (2024) 8:100446. doi: 10.1016/j.chphi.2023.100446
- 72. Grafmüller J, Böhm A, Zhuang Y, Spahr S, Müller P, Otto TN, et al. Wood ash as an additive in biomass pyrolysis: effects on biochar yield, properties, and agricultural performance. *ACS Sustain Chem Eng.* (2022) 10:2720–9. doi: 10.1021/acssuschemeng.1c07694
- 73. Da TX, Ren HK, He WK, Gong SY, Chen T. Prediction of uranium adsorption capacity on biochar by machine learning methods. *J Environ Chem Eng.* (2022) 10:108449. doi: 10.1016/j.jece.2022.108449
- 74. Jiang S, Hou Y, Man Z, Wang C, Shi X, Shang J, et al. Guiding experiment with Machine Learning: A case study of biochar adsorption of Ciprofloxacin. *Sep Purif Technol.* (2024) 334:126023. doi: 10.1016/j.seppur.2023.126023
- 75. Zhu X, Wang X, Ok YST. The application of machine learning methods for prediction of metal sorption onto biochars. *J Hazard Mater.* (2019) 378:120727. doi: 10.1016/j.jhazmat.2019.06.004

- 76. Tan X, Zhu S, Wang R, Chen Y, Show PL, Zhang F, et al. Role of biochar surface characteristics in the adsorption of aromatic compounds: pore structure and functional groups. *Chin Chem Lett.* (2021) 32:2939–46. doi: 10.1016/j.cclet.2021.07.042
- 77. Du Z, Sun X, Zheng S, Wang S, Wu L, An Y, et al. Optimal biochar selection for cadmium pollution remediation in Chinese agricultural soils via optimized machine learning. *J Hazard Mater.* (2024) 476:135065. doi: 10.1016/j.jhazmat.2024.135065
- 78. Melo V, GF F, Fregolente LV. Sustainable catalysts for biodiesel production: The potential of CaO supported on sugarcane bagasse biochar. *Renew Sustain Energy Rev.* (2024) 189:114042. doi: 10.1016/j.rser.2023.114042
- 79. Jaffari ZH, Jeong H, Shin J, Kwak J, Son C, Lee Y-G, et al. Machine-learning-based prediction and optimization of emerging contaminants' adsorption capacity on biochar materials. *Chem Eng J.* (2023) 466:143073. doi: 10.1016/j.cej.2023.143073
- 80. Xu S, Yuan JY, Zhang YT, Yang QL, Zhang CX, Guo Q, et al. Effects of different precursors on the structure of lignin-based biochar and its ability to adsorb benzopyrene from sesame oil. *Int J Biol Macromol.* (2024) 269:132216. doi: 10.1016/j.ijbiomac.2024.132216
- 81. Zhang Y, Qin J, Yi Y. Biochar and hydrochar derived from freshwater sludge: Characterization and possible applications. *Sci Total Environ*. (2021) 763:144550. doi: 10.1016/j.scitotenv.2020.144550
- 82. Ahmed MJ, Hameed BH. Insight into the co-pyrolysis of different blended feedstocks to biochar for the adsorption of organic and inorganic pollutants: A review. *J Clean Prod.* (2020) 265:121762. doi: 10.1016/j.jclepro.2020.121762
- 83. Wijitkosum S, Sriburi T. Aromaticity, polarity, and longevity of biochar derived from disposable bamboo chopsticks waste for environmental application. *Heliyon*. (2023) 9:e19831. doi: 10.1016/j.heliyon.2023.e19831
- 84. Song Y, Huang Z, Jin M, Liu Z, Wang X, Hou C, et al. Machine learning prediction of biochar physicochemical properties based on biomass characteristics and pyrolysis conditions. *J Anal Appl Pyrolysis*. (2024) 181:106596. doi: 10.1016/j.jaap.2024.106596
- 85. Yin Y, Yang C, Li M, Zheng Y, Ge C, Gu J, et al. Research progress and prospects for using biochar to mitigate greenhouse gas emissions during composting: A review. *Sci Total Environ*. (2021) 798:149294. doi: 10.1016/j.scitotenv.2021.149294
- 86. Sinha R, Kumar R, Sharma P, Kant N, Shang J, Aminabhavi TM. Removal of hexavalent chromium via biochar-based adsorbents: State-of-the-art, challenges, and future perspectives. *J Environ Manage*. (2022) 317:115356. doi: 10.1016/j.jenvman.2022.115356
- 87. Supraja KV, Kachroo H, Viswanathan G, Verma VK, Behera B, Doddapaneni TRKC, et al. Biochar production and its environmental applications: Recent developments and machine learning insights. *Bioresour Technol.* (2023) 387:129634. doi: 10.1016/j.biortech.2023.129634
- 88. Inyang MI, Gao B, Yao Y, Xue Y, Zimmerman A, Mosa A, et al. A review of biochar as a low-cost adsorbent for aqueous heavy metal removal. *Crit Rev Environ Sci Technol.* (2016) 46:406–33. doi: 10.1080/10643389.2015.1096880
- 89. Rahman MZ, Edvinsson T, Kwong P. Biochar for electrochemical applications. Curr Opin Green Sustain Chem. (2020) 23:25–30. doi: 10.1016/j.cogsc.2020.04.007
- 90. Tiwari SK, Bystrzejewski M, De Adhikari A, Huczko A, Wang N. Methods for the conversion of biomass waste into value-added carbon nanomaterials: Recent progress and applications. *Prog Energy Combust Sci.* (2022) 92:101023. doi: 10.1016/j.pecs.2022.101023
- 91. Basha DB, Ahmed S, Ahmed A, Gondal MA. Recent advances on nitrogen doped porous carbon micro-supercapacitors: New directions for wearable electronics. *J Energy Storage*. (2023) 60:106581. doi: 10.1016/j.est.2022.106581
- 92. Wang L, Hu X. Recent advances in porous carbon materials for electrochemical energy storage. *Chem Asian J.* (2018) 13:1518–29. doi: 10.1002/asia.201800553
- 93. Xi Y, Liu X, Xiong W, Wang H, Ji X, Kong F, et al. Converting amorphous kraft lignin to hollow carbon shell frameworks as electrode materials for lithium-ion batteries and supercapacitors. *Ind Crops Prod.* (2021) 174:114184. doi: 10.1016/j.indcrop.2021.114184
- 94. Leng L, Yang L, Leng S, Zhang W, Zhou Y, Peng H, et al. A review on nitrogen transformation in hydrochar during hydrothermal carbonization of biomass containing nitrogen. *Sci Total Environ*. (2021) 756:143679. doi: 10.1016/j.scitotenv.2020.143679
- 95. Cao H, Milan YJ, Mood SH, Ayiania M, Zhang S, Gong X, et al. A novel elemental composition based prediction model for biochar aromaticity derived from machine learning. *Artif Intell Agric.* (2021) 5:133–41. doi: 10.1016/j.aiia.2021.06.002
- 96. Palansooriya KN, Li J, Dissanayake PD, Suvarna M, Li L, Yuan X, et al. Prediction of soil heavy metal immobilization by biochar using machine learning. *Environ Sci Technol.* (2022) 56:4187–98. doi: 10.1021/acs.est.1c08302
- 97. Zhu X, Li Y, Wang X. Machine learning prediction of biochar yield and carbon contents in biochar based on biomass characteristics and pyrolysis conditions. *Bioresour Technol.* (2019) 288:121527. doi: 10.1016/j.biortech.2019.121527
- 98. Nidheesh PV, Kumar M, Venkateshwaran G, Ambika S, Bhaskar S, Vinay, et al. Conversion of locally available materials to biochar and activated carbon for drinking water treatment. *Chemosphere*. (2024) 353:141566. doi: 10.1016/j.chemosphere.2024.141566
- 99. Ifthikar J, Ibran Shahib I, Jawad A, Gendy EA, Wang S, Wu BB, et al. The excursion covered for the elimination of chromate by exploring the coordination

mechanisms between chromium species and various functional groups. Coord Chem Rev. (2021) 437:213868. doi: 10.1016/j.ccr.2021.213868

- 100. Zhu X, Xu Z, You S, Komárek M, Alessi DS, Yuan X, et al. Machine learning exploration of the direct and indirect roles of Fe impregnation on Cr(VI) removal by engineered biochar. *Chem Eng J.* (2022) 428:131967. doi: 10.1016/j.cej.2021.131967
- 101. Xu Z, Xu X, Zhang Y, Yu Y, Cao X. Pyrolysis-temperature depended electron donating and mediating mechanisms of biochar for Cr(VI) reduction. *J Hazard Mater.* (2020) 388:121794. doi: 10.1016/j.jhazmat.2019.121794
- 102. Chen Y, Qian Y, Ma J, Mao M, Qian L, An D. New insights into the cooperative adsorption behavior of Cr(VI) and humic acid in water by powdered activated carbon. *Sci Total Environ.* (2022) 817:153081. doi: 10.1016/j.scitotenv.2022.153081
- 103. Tang Z, Kong Y, Zhao S, Jia H, Vione D, Kang Y, et al. Enhancement of Cr(VI) decontamination by irradiated sludge biochar in neutral conditions: Evidence of a possible role of persistent free radicals. *Sep Purif Technol.* (2021) 277:119414. doi: 10.1016/j.seppur.2021.119414
- 104. Holanda MAS, Coelho Menezes JM, Coutinho HDM, Teixeira RNP. Effectiveness of biochar as an adsorbent for pesticides: Systematic review and meta-analysis. *J Environ Manage*. (2023) 345:118719. doi: 10.1016/j.jenvman.2023.118719
- 105. Pathy A, Pokharel P, Chen X, Balasubramanian P, Chang SX. Activation methods increase biochar's potential for heavy-metal adsorption and environmental remediation: A global meta-analysis. *Sci Total Environ*. (2023) 865:161252. doi: 10.1016/j.scitotenv.2022.161252